TRIBHUVAN UNIVERSITY

INSTITUTE OF ENGINEERING

PULCHOWK CAMPUS

THESIS NO: S007/075

SEISMIC VULNERABILITY OF RC FRAME BUILDING WITH VARIATION IN EFFECTIVE STIFFNESS

by

Namrata Thapa

A THESIS

SUBMITTED TO THE DEPARTMENT OF CIVIL ENGINEERING IN PARTIAL FULFILLMENT OF THE REQUIREMENTS FOR THE DEGREE OF MASTER OF SCIENCE IN STRUCTURAL ENGINEERING

DEPARTMENT OF CIVIL ENGINEERING

LALITPUR, NEPAL

SEPTEMBER, 2021

COPYRIGHT

CERTIFICATION OF APPROVAL

TRIBHUVAN UNIVERSITY

INSTITUTE OF ENGINEERING

DEPARTMENT OF CIVIL ENGINEERING

PULCHOWK CAMPUS

The undersigned certify that they have read, and recommended to the Institute of Engineering for acceptance, a thesis entitled, "**Seismic Vulnerability of RC Frame Building with Variation in Effective Stiffness**" submitted by Ms. Namrata Thapa (075/MSStE/007) in partial fulfillment of requirement for the degree of Master of Science in Structural Engineering.

Supervisor, Prof. Dr. Prem Nath Maskey

Department of Civil Engineering

Institute of Engineering

Pulchowk Campus

External Examiner, Er. Binay Charan Shrestha

Program Coordinator, Prof. Dr. Kamal Bahadur Thapa

Department of Civil Engineering

Institute of Engineering

Pulchowk Campus

Date:

ABSTRACT

Due to cracking, there will be a substantial reduction in flexural stiffness which ultimately results in larger deflections. Member stiffness is commonly considered as the gross stiffness, or as the effective stiffness which is an approximate percentage of gross stiffness, in the study and design of reinforced concrete (RC) buildings. NBC 105:2020 recommends the use of effective stiffness of cracked sections during analysis, however it is not addressed in NBC 105:1994. Several configurations of moment-resisting frames, regular in plan and elevation, with variation in the number of bays and storey number are designed and analyzed by using gross and cracked section properties. The motive of this research is to study the effect of the modeling approach of building in terms of gross and cracked sections on the structural performance under earthquakes. Non-linear static analysis is done in ETABSv19 to evaluate the overstrength and ductility of structures designed using gross and cracked section properties.

ACKNOWLEDGEMENT

I take this opportunity as a privilege to thank all the individuals without whose support and guidance I could not have completed this thesis in the stipulated period of time. First and foremost, I would like to express my deepest gratitude to my respected supervisor Prof. Dr. Prem Nath Maskey for his invaluable support, guidance, motivation and encouragement throughout the research period. His readiness for consultation at all times, his insightful comments and inputs, his concern and assistance even with practical things have been extremely beneficial.

I would also like to acknowledge all the faculty members of the Department of Civil Engineering for imparting their knowledge and valued inputs during my study at IOE, Pulchowk Campus.

Finally, I wish to thank my family who encouraged me every day to keep on striving towards my goal. Their words of support gave the much-needed motivation to persevere in the hardest of times.

TABLE OF CONTENTS

LIST OF TABLES

LIST OF FIGURES

LIST OF SYMBOLS AND ACRONYMS

ASCE	American Society of Civil Engineers
ACI	American Concrete Institute
Ω	Overstrength Factor
DL	Dead Load of the structure
LL	Live load
NBC	Nepal National Building Code
NZS	New Zealand Standards
I	Importance Factor
IS	Indian Standard
R_μ	Ductility Factor
S	Number of Storey
B	Number of Bays
W	Total Seismic Weight of the structure
V_d	Design Base Shear
V_y	Significant Yield Strength
Z	Seismic Zoning factor
λ	Live load participation factor
Φ	Function of soil condition
μ	Displacement ductility ratio

CHAPTER 1: INTRODUCTION

1.1 Introduction

Cracking is an inevitable phenomenon in concrete structures resulting from various factors like applied loads, shrinkage, thermal load and settlement. When the tensile stress of a certain element increases beyond rupture stress, there will be cracking and that particular element will not have the same stiffness as it used to have prior to cracking. It would be ideal if the stiffness of each member reflected the degree of cracking caused by applied loads.

As a result of cracking, flexural stiffness will be significantly reduced. The lateral deflection of reinforced concrete members increases as the flexural stiffness value decreases, and it can be far more than the deflection anticipated using gross flexural stiffness. It is very crucial to estimate the flexural stiffness of individual components so as to capture the dynamic properties of a structure as well as the force versus deformation demands. The parameters like time period, deflection, internal force distribution and overall dynamic response of the structure are affected due to change in stiffness. Therefore, it is essential to use the reduced or effective stiffness of the reinforced concrete structure. It is practically impossible to retain the uncracked stiffness of a structural member during or after a seismic response. Thus, it can be inferred that uncracked stiffness is not an accurate estimate of the effective stiffness. Moreover, using uncracked stiffness results in inaccurate estimation of seismic forces as well as incorrect force distribution across the structure (Priestley, 2003).

To take these effects into consideration, the design code of several countries suggests some reduction factors or equations to reduce the gross stiffness to effective stiffness. In Nepal National Building Code NBC 105:1994, there were no provisions to account for the reduction in stiffness due to concrete cracking. However, the new revised NBC 105:2020 recommends effective moment of inertia of 70% of I_{gross} of columns and 35% of I_{gross} of beams for the analysis of RC frame structures. The value of effective moment of inertia of columns is higher than that of beams because damage expected in columns is lower owing to presence of compressive axial load in them (Murty et al., 2012). Furthermore, a rational analysis is suggested to estimate the elastic flexural and shear stiffness properties of cracked concrete.

1.2 Need of Study

NBC 105:2020 is a recently updated code, and since it is still in its initial implementation phase, the response of this code on various aspects like design output, the structural performance of the building, etc. are not entirely known. Some principal modifications made in the code are load factor, load combination, performance definition, return period, seismic zone map, importance class, spectral shape factor, the formulation for horizontal base shear coefficient and the use of cracked section for analysis. In NBC 105:1994, the analysis was done assuming gross section while NBC 105:2020 suggests the use of cracked section during analysis which are presented in terms of the effective stiffness of cracked sections in Table 2-2.

Hence, to get an insight about the effects of using cracked and gross section properties during analysis, the present study is needed. This study will provide insights into the design output, structural performance, and some other salient features of the selected class of buildings designed and analyzed as per NBC 105:2020. Also, this research could act as a reference for updating NBC 205:1994 (Mandatory rules of thumb reinforced concrete buildings without masonry infill) as per the new revised code.

1.3 Objectives of the Study

1. To develop the fragility curves for RC Frame buildings designed using Gross and Cracked section.
2. To compare the results of the seismic assessment of RC frame building designed using Gross and Cracked section.
3. To compare the overstrength and ductility factor of RC frame building designed using Gross and Cracked section.

1.4 Methodology

This section describes the methodology followed to achieve the above-mentioned objectives.

1. Review of code provisions for the effective moment of inertia of beams and columns suggested in various international standards and available literature related to overstrength and ductility. Survey and review of various literature available to related works.
2. Selection of parameters to be considered for fictitious RC framed building. (Building geometry, material properties, etc.)

3. Finite element modeling of the building using ETABS. Each building will be designed using both gross and cracked sections and an equivalent linear static analysis will be performed initially, followed by nonlinear static analysis.
4. Calculation of overstrength and ductility factor. Seismic Vulnerability Assessment will be done using HAZUS methodology and the output will be presented in terms of fragility curves.
5. Results will be compared and discussed.

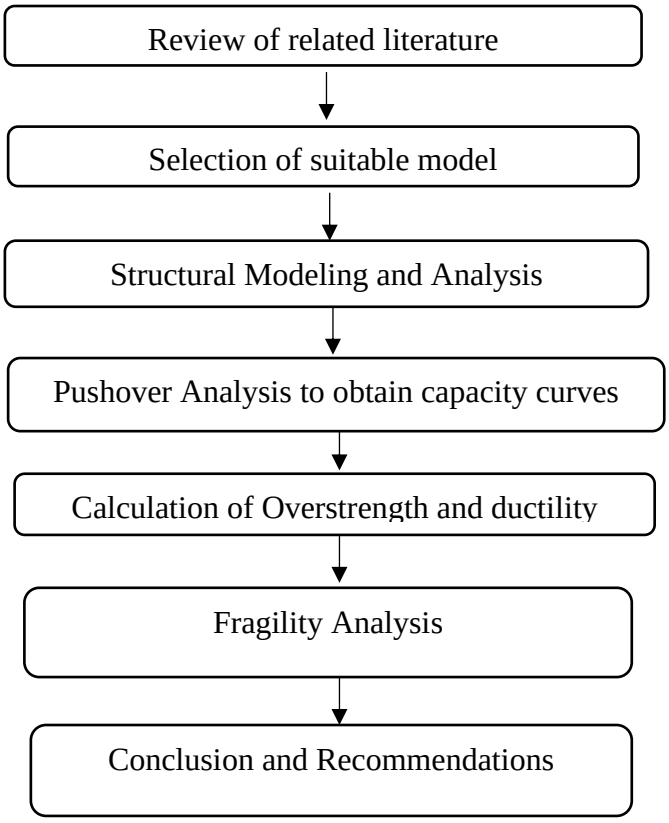

Figure 1-1 Flow chart of methodology

1.5 Thesis Organization

This thesis work has been presented in six chapters. The introductory chapter gives a brief overview about the cracking phenomenon in concrete and why it should be considered during the analysis of structures. The need of study, objectives of the research work as well as the methodology are identified.

Chapter 2 contains the review of various international code provisions regarding the stiffness reduction factors. This will also include the literature review for gross and cracked section, overstrength and ductility factors and fragility analysis.

Chapter 3 presents the theoretical background regarding gross and cracked section properties as well as stiffness reduction values obtained from various laboratory experiments. This chapter also describes the methods of structural analysis focusing mainly on the non-linear static analysis.

Chapter 4 contains the description of selected buildings and structural modeling parameters.

Chapter 5 presents the results obtained from the nonlinear analysis of the building models. This chapter also presents the results by comparing the analysis results obtained for the building designed using gross as well as cracked section.

Chapter 6 sums up the conclusions drawn from the results obtained. The scope of future work is also discussed.

References used in this research work are listed followed by the appendix that contains the results in tabular form for various models considered in this research work.

CHAPTER 2: REVIEW OF CODE PROVISIONS AND LITERATURE

2.1 Code provisions for effective moment of inertia

The seismic design codes of various countries have their own recommendations for the effective moment of inertia. An overview of code provisions for seismic load calculation of some countries is presented in this section. Some of the codes that have been referred to in this study are listed below:

a. NBC 105: 2020
b. IS 1893:2016
c. Turkish Building Code (2018)
d. ASCE 41-13 (2013)
e. AIJ Standard for Structural Calculation of RC Structures (2010)
f. NZS 3101: Part 2 (2006)
g. Eurocode-8 (2005)
h. ACI 318-19 (2019)
i. FEMA 356 (2000)

Table 2-1 Effective moment of inertia of beams and columns suggested in different international standards.

Codes	**Beams**	**Columns**	**Wall uncracked**	**Wall cracked**
NBC 105:1994	No Provision			
IS 1893:2016	0.35 I_g	0.70 I_g	-	-
NZS 3101	0.35 I_g - 0.4 I_g	0.40 I_g - 0.80 I_g	n/a	0.32 I_g - 0.48 I_g
ACI 318-19	0.35 I_g	0.7 I_g	0.7 I_g	0.5 I_g
Eurocode-8	0.5 I_g	0.5 I_g	0.5 I_g	0.5 I_g
ASCE 41-13	0.30 I_g	0.7 I_g	n/a	0.5 I_g
FEMA 356	0.5 I_g	0.5 I_g - 0.7 I_g	0.8 I_g	0.5 I_g

2.1.1 NBC 105:2020

NBC 105:1994 was silent about the effective moment of inertia for structural members. However, the new revised NBC 105:2020 stipulates the use of the effective moment of inertia in the form of reduction factors as shown in the table below.

Table 2-2 Effective stiffness of different components (NBC 105:2020)

S.No.	Component	Flexural stiffness	Shear stiffness
1.	Beams	$0.35\ E_cI_g$	$0.40\ E_cA_w$
2.	Columns	$0.70\ E_cI_g$	$0.40\ E_cA_w$
3.	Wall un-cracked	$0.80\ E_cI_g$	$0.40\ E_cA_w$
4.	Wall cracked	$0.50\ E_cI_g$	$0.40\ E_cA_w$

2.1.2 IS 1893:2016

As per IS 1893:2016 clause 6.4.3.1, the effective moment of inertia (I_{eff}) for the beam is suggested to be $0.35\ I_{gross}$ and $0.70\ I_{gross}$ for the column.

Where, Gross moment of inertia $I_{gross} = \frac{bh^3}{12}$

b= width of the member

h= height or depth of the member

2.1.3 Turkish Building Earthquake Code (2018)

The suggested effective stiffness in the Turkish Building Earthquake Code (2018) is given in the table below:

Table 2-3 Effective stiffness of different members (TBEC 2018)

Concrete Member	Flexural Stiffness	Shear Stiffness
Beam	0.35	1.00
Column	0.70	1.00
Wall (equivalent strut)	0.50	0.50

2.1.4 ASCE 41-13 (2013)

In ASCE 41-13, the flexural rigidity of columns is related to axial load. The effective rigidity of beams and shear walls are constant whereas the effective rigidity for columns relies on the applied axial load. It distinguishes between columns with axial load more

than or less than $0.1*A_g*f_c'$. For further information on calculating the effective stiffness of reinforced concrete columns, reference to Elwood and Eberhard (2009) is recommended.

2.1.5 AIJ (2010)

AIJ (2010) differs from U.S. standards in its approach regarding effective stiffness as it incorporates the empirical equations developed by Sugano (1970) to define the element effective moment of inertia:

$$I_{eff} = \alpha_y I_g \tag{2.1}$$

$$\alpha_y = \left(0.043 + 1.64\eta\rho_t + 0.043\frac{a}{h} + 0.33\eta\right)\left(\frac{d}{h}\right)^2 \tag{2.2}$$

For columns and beams:

I_g= gross moment of inertia

h = overall depth of the section

η = modular ratio of steel to concrete

ρ_t = longitudinal reinforcement ratio calculated as the area of longitudinal steel divided by the cross-sectional area.

d = effective depth of the section

2.1.6 NZS 3101: Part 2 (2006)

NZS 3101: Part 2 (2006) stipulates that effective rigidity of the concrete members is influenced by the level of cracking, the tensile strength of the concrete, amount of reinforcement and the initial conditions in the member. The standard includes recommended effective rigidities for different members comparable to US codes to ease the extensive analysis required for addressing these issues. The load level in NZS 3101, however, varies from U.S. codes.

For beams, I_{eff} = 0.35 I_g-0.40 I_g

For columns, I_{eff} = 0.40 I_g-0.8 I_g

2.1.7 Eurocode 8 (2005)

As per Eurocode 8, the elastic stiffness of the bilinear force-deformation relation in reinforced concrete elements should correspond to that of cracked sections and the onset of reinforcement yielding. In Eurocode8, the effective flexural rigidity of all members is assumed to be half of the gross flexural rigidity.

2.1.8 ACI 318-19 (2019)

In ACI 318-19, the gross section flexural rigidity E_cI_g is reduced to obtain the effective flexural rigidity E_cI_{eff} which compensates for cracking and other softening effects. The gross-section flexural rigidity was reduced in the computational model by a factor of 0.7 for columns, 0.5 or 0.7 for walls, and 0.35 for beams. ACI 318-19 additionally allows for the use of a flexural rigidity reduction factor of 0.5 for all members.

Table 2-4 Effective moment of inertia (ACI 318-19)

Member	Minimum	Alternative value of I	Maximum
Columns and walls	$0.35I_g$	$\left(0.80 + 25\frac{A_{st}}{A_g}\right)\left(1 - \frac{M_u}{P_u h} - 0.5\frac{P_u}{P_o}\right)I_g$	$0.875I_g$
Beams, flat plates and flat slabs	$0.25I_g$	$(0.10 + 25\rho)\left(1.2 - 0.2\frac{b_w}{d}\right)I_g$	$0.5I_g$

Where, A_g is the area of the gross section;

A_{st} is the area of reinforcing steel;

I_g is the moment of inertia of the gross uncracked section with respect to the central axis;

P_u is the ultimate load in compression;

d is the effective height of the section.

2.1.9 FEMA 356 (2000)

$$EI_{eff} = \frac{M_{0.004}L^2}{6\,\Delta_y} \qquad 2.3$$

where Δ_y is the yield displacement of the column taking into account the displacement due to flexure, bar slip and shear.

2.2 Areas on which the literatures were reviewed

2.2.1 Literature related to Gross and Cracked section

Priestley (2003) pointed out that performing modal analysis with uncracked section stiffness for different elements makes obtaining precise seismic forces, even within the elastic range, impossible. Computed elastic periods are most likely incorrect and force distribution across the structure, which is dependent on the relative stiffness of the elements, may be overly inaccurate.

Elwood and Eberhard (2009) concluded that the stiffness of the structural elements had a significant impact on the calculated response of the structure subjected to ground motion. Member stiffness regulates predictions of the period of the structure, load distribution within the structure, and deformation demand in the linear analysis of members. In order to estimate the yield displacement correctly in nonlinear analysis, an accurate assessment of the member stiffness was required, which in turn affected the expected displacement ductility demands.

Ahmed (2008) investigated how concrete cracking affects the lateral response of building structures. He also discussed controversies in the formulation of the parameter related to reinforced concrete cracking. With concrete cracking considered, a large increase in deflection was seen, with an average 50% increase in top storey absolute deflections and an estimated 40% increase in drifts. He also concluded that given the current country code standards, which make no mention of effective rigidity, the drift requirements may fail following the incorporation of the concrete cracking effect.

Pique and Burgos (2008) highlighted the ease with which the effective stiffness of elements can be considered. He inferred that although most seismic standards accept inelastic incursions, they do not establish effective stiffness for seismic analysis. He concluded that cracking must be taken into account in seismic analysis of structures in order to provide realistic distortions in the nonlinear range since these are computed using an elastic analysis. In the case of seismic analysis with uncracked sections, design moments were larger than in the other two assessed approaches, allowing for a conservative design in strength but larger distortions.

Kaushik and Mane (2010) analytically studied the effect of the cracked section on lateral response of RC structure. A variety of columns were studied in this study by

varying numerous characteristics such as grade of concrete and steel, percentage of steel, axial load, and section size changes in flexural stiffness (EI) with various parameters taken into account. The result suggested that IS 1893:2002 seismic code had no provision to deal with this effect. However, in seismic codes of several other countries, some reduction factors or equations are proposed to reduce the gross stiffness of RC members to effective stiffness.

Kaushik (2011) investigated the significance of effective stiffness properties of RC members in seismic analysis and design of structures. The parametric study involved about eleven thousand beam and column sections. The lateral deflections of the structure surpassed the drift limits provided in the seismic codes due to the reduction in EI of beams and columns. Through his analytical study, he proposed a simple equation for the estimation of realistic values of cracked section properties of reinforced concrete beams and columns.

Surana et al. (2015) conducted a seismic performance assessment on mid-rise RC frame and Frame-shear wall buildings designed for Indian codes. An RC frame structural system with two separate models was taken, one with gross RC section properties and the second with cracked section properties as per ASCE 41 guidelines. The results showed that frame buildings designed only for force criterion had lower ductility capacity than frame buildings designed for force and drift criterion.

Kwon and Ghannoum (2016) investigated the accuracy of stiffness provisions of American, Japanese, Canadian, New Zealand, and European standards. The findings suggested improvements in the stiffness provisions of all investigated standards for concrete buildings. At low drift levels, the lateral stiffness of the test structure was shown to diminish significantly, which was primarily due to concrete cracking. He also concluded that all standard stiffness values were higher than those of the building at the drift target of the standard.

Prajapati and Amin (2019) performed a comparative seismic assessment of RC frame building designed using uncracked and cracked section as per Indian standards. The results showed that the inter-storey drift of RC frames designed using gross section properties is within the permissible limit, whereas the inter-storey drift of RC frames

designed using effective section properties for the force criteria alone is much higher and exceeds the maximum permissible inter-storey drift ratio.

2.2.2 Literature related to Overstrength and Ductility factor

Chaulagain et al. (2014) calculated the response reduction factor of irregular RC buildings in Kathmandu Valley. A total of twelve building models were used in the study in which existing engineered buildings in Kathmandu valley were considered. They concluded that buildings with a complete load path and which satisfy the column beam capacity ratio of 1.1 have a higher value of response reduction factor. If the overstrength factor has a higher value then the overall response reduction factor can be attained even if the ductility factor is less.

Rajbhandari (2019) performed a study to evaluate the effect of size of building on response reduction factor for low rise residential buildings. Nonlinear static analysis was performed wherein the number of storeys, size of bays as well as the number of bays were varied. The final output of this study was presented in terms of an empirical formula which if not precisely, closely predicts the value of overstrength and ductility.

Miranda (1993) conducted a study on the usage of site-dependent reduction factors to minimize the elastic design spectra of structures. The effectiveness of using strength reduction factors to reduce the linear elastic design spectrum of structures was investigated. The statistical study demonstrated that for certain structures, the use of period-independent reduction factors is insufficient and the different types of soil conditions can have an impact on the strength reduction factors.

2.2.3 Literature related to Fragility Analysis

Calvi et al. (2006) reviewed the development of various vulnerability assessment methodologies over the past 30 years and also presented the major advantages and drawbacks of each methodology. He inferred that the ideal approach for the future needs to be a blend of the positive aspects of different vulnerability assessment methodologies.

Haldar and Singh (2009) carried out research on the seismic performance and vulnerability of RC frame buildings designed as per the Indian provisions. In this study, existing 4-story and 9-story RC hospital buildings in New Delhi were studied which were designed as per the force-based design philosophy. FEMA-440 and HAZUS methodologies were used to compare the performance and vulnerability of the SMRF and OMRF buildings. Results showed that, because of the higher permissible ultimate drift limit, SMRF buildings are more vulnerable than the OMRF building.

Halder and Paul (2016) assessed the seismic vulnerability of low-rise RC frame building which is designed for gravity loads in accordance to the Indian code. Based on HAZUS methodology, fragility curves for various damage grades were developed. Damage probability matrices (DPM) were developed for two different seismic hazard levels, namely the maximum considered earthquake and the design basis earthquake, based on the performance point, in order to compare the damage state for each hazard level. The results revealed that the damage to the considered building ranged from moderate to severe depending on the seismic hazard level.

CHAPTER 3: THEORETICAL FORMULATION

3.1 Gross and Cracked section

Basically, there are two approaches that can be adopted for the design of concrete structures i.e., gross and cracked section. In an uncracked section, the member is loaded up to the point of cracking but remains uncracked and the stress distribution is assumed to be linear whereas in the case of cracked section non-linear stress distribution is assumed.

Gross Section

The bending tensile stress in concrete is minimal when the value of the applied moment is small. As a result, the applied moment in an uncracked section is less than the cracking moment (M_{cr}), and the tensile stress is less than the flexural tensile strength (f_{cr}). This is referred to as the uncracked phase, and it occurs when the entire section is effective in resisting the moment and is under stress. The level of cracking is anticipated to be minimal in this case. The strain across the cross-section is minor because the moment is small and does not cause cracking, and the neutral axis lies at the centroid. It is important to replace the reinforced concrete cross-section with an equivalent, transformed section to determine the stresses in an uncracked section. For that purpose, steel is replaced with an equivalent amount of concrete. As steel has a significantly higher modulus of elasticity than concrete, the area of steel is substituted by a much larger area of concrete.

Cracked Section

In the case of cracked section, the value of applied moment exceeds the cracking moment (M_{cr}) which results in the appearance of cracks in the tension zone of the concrete member as a result of which the concrete is unable to withstand tension anymore. Any further increase in the applied moment must be accounted for entirely by the reinforcing steel. The comparatively large increase in the tensile strain of reinforcements causes the neutral axis to shift upward. The deflection and rotation increase at a higher pace, resulting in a faster increase in curvature. The crack initiates at the bottom and gradually expands and progresses towards the neutral axis as the stress increases.

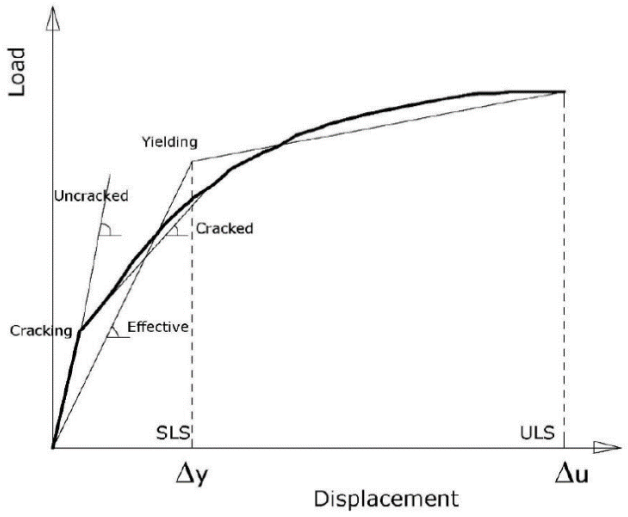

Figure 3-1 Load displacement plot of RC members (NBC 105:2020)

3.2 Previous Studies and Equations proposed for effective moment of inertia

The concept of effective moment of inertia was originally conceived by Branson (1965) in which the main idea was to consider the moment of inertia in such a way that it incorporated the effects of cracking. Most of the aforementioned studies and many others have formed the basis of codes and guidelines.

Branson (1965)

Branson (1965) was a pioneer in dealing with the problems involving the estimation of stiffness in cracked regions. His work was used as a reference in (ACI-318 2002). The effective moment of inertia (I_e) approach introduced by Branson allows for a gradual shift from uncracked to cracked transformed section as the ratio of service load moment M_a to cracking moment M_{cr} increases.

$$I_e = \left(\frac{M_{cr}}{M_a}\right)^3 . I_g + \left[1 - \left(\frac{M_{cr}}{M_a}\right)^3\right] . I_{cr} \leq Ig \qquad 3.1$$

where M_{cr} and M_a are cracking and SLS applied moment respectively;

I_g is the moment of inertia of the gross section and I_{cr} is the first cracking moment of inertia of the gross section.

Sugano (1970)

Sugano (1970) proposed a reduced stiffness for beams and columns based on multiple experimental results and the ratio of secant stiffness at yielding to gross uncracked section stiffness.

$$\frac{K_r}{K_i} = \left(0.043 + 1.64\eta\rho_t + 0.043\frac{a}{h} + 0.33\eta\right)\left(\frac{d}{h}\right)^2 \qquad 3.2$$

Limitations:

$0.4 < \rho_t < 2.8\%$

$2 < \frac{a}{h} < 5$

$0 < \frac{P}{A_g f_c'} < 0.55$

where K_r/K_i is the ratio between the secant stiffness at yielding and the initial stiffness of the member; $\eta = \frac{P}{A_g f_c'}$ is the normalized axial stress.

Grossman (1981)

In 1981, Grossman proposed to compute the stiffness of cracked beams exposed to bending using the ratio of the first cracking moment M_{cr} to the applied moment M_a. He also proposed a parametric parameter K_e for large moment values, which is affected by the mechanical characteristics of concrete and steel. Grossman estimated the approximate value of I_e without knowing the area of flexure reinforcement.

For $M_a/M_{cr} \leq 1.6$

$$I_e = \left(\frac{M_a}{M_{cr}}\right)^4 . I_g \leq I_g \qquad 3.3$$

For $1.6 < M_a/M_{cr} \leq 10$

$$I_e = 0.1K_e\left(\frac{M_a}{M_{cr}}\right)^4 . I_g \leq I_g \qquad 3.4$$

Where M_{cr} and M_a are cracking and SLS applied moment respectively and K_e is a factor depending on the density of concrete and grade of steel but I_e should not be less than $0.35\ K_e . I_g$

Wang (2001)

In 2001, Wang suggested a revised Branson's method for beams in bending.

When $M_{cr} \leq M_s$

$$I_e = \left(\frac{2M_{cr}{}^2}{M_a^2 + M_s^2}\right).I_g + \left[1 - \left(\frac{2M_{cr}{}^2}{M_a^2 + M_s^2}\right)\right].I_{cr} \quad 3.5$$

When $M_s \leq M_{cr} \leq M_a$

$$I_e = \left(\frac{M_a + M_s}{M_a + M_s}\right).I_g + \left[1 - \left(\frac{2M_{cr}}{M_a + M_s}\right)\right].I_{cr} \quad 3.6$$

When $M_{cr} \geq M_a$

$$I_e = I_g \quad 3.7$$

Where, M_s is the maximum bending moment due to short term loads and M_{cr} and M_a are cracking and SLS applied moment respectively.

Mehanny (2001)

Mehanny (2001) also established a value for the effective stiffness based on the area of the reinforcement. He proposed simple methods for determining the effective flexural and shear stiffness coefficients of beams and columns when the axial load level is taken into account. He also proposed a revised EI_{eff} value based on the applied axial compression load.

$$\frac{EI_{eff}}{EI_{g,tr}} = \left(0.4 + \frac{P}{2.4P_b}\right) \leq 0.9 \quad 3.8$$

Where P_b is the normal action for balanced failure; P is the design normal load.

Khuntia and Ghosh (2004)

Khuntia and Ghosh (2004) focused on the evaluation of the effective stiffness of RC frames subjected to lateral loads by adding a new parameter i.e., the steel ratio. The effective stiffness EI_{eff} of an RC column under seismic or wind loads was also proposed, as was a simplified equation for RC beams cast with normal-strength concrete and another for high-performance or high-strength concrete. They also suggested simple effective stiffness models to be employed in the lateral analysis of frames in general

and with slender columns, considering the role of longitudinal reinforcement and eccentricity of the axial load.

$$EI_{eff} = E_c I_g (0.8 + 0.25\rho_c)\left(0.30 + 0.5\frac{P}{P_u}\right) \leq E_c I_c \ \& \ \geq E_c I_{beam} \quad 3.9$$

$$EI_{eff} = E_c I_g (0.10 + 25\rho_b)\left(1.2 - 0.2\frac{b}{h}\right) \leq 0.6 E_c I_g \quad 3.10$$

$$EI_{eff} = E_c I_g (0.10 + 25\rho_b)\left(1.2 - 0.2\frac{b}{h}\right)(1.15 - 0.00004 f_c') \leq 0.6 E_c I_g \quad 3.11$$

Limitations:

$\left(1.2 - \frac{0.2b}{h}\right) \leq 1$

$P_u = 0.85 f_c'(A_g - A_{st}) + f_y A_{st}$

where b is the width of the rectangular section; f_c' is the compressive strength of concrete; h is the height of the cross-section; E_c is the elastic modulus of concrete and P_u is the ultimate load in compression.

Elwood and Eberhard (2009)

Elwood and Eberhard (2009) provided the values to lower the stiffness for RC columns with rectangular cross-sections in RC frames under seismic loading based on the findings of their tests. A general equation for rectangular and circular columns was developed, neglecting the reinforcement ratio in the cross-section.

For Rectangular columns

For $\frac{P}{A_g f_c'} \leq 0.2$

$$\frac{EI_{eff}}{EI_g} = 0.2 \quad 3.12$$

For $0.2 < \frac{P}{A_g f_c'} \leq 0.5$

$$\frac{EI_{eff}}{EI_g} = \frac{5P}{3A_g f_c} - \frac{4}{30} \quad 3.13$$

For $0.5 < \frac{P}{A_g f_c'}$

$$\frac{EI_{eff}}{EI_g} = 0.7 \quad 3.14$$

For rectangular and circular columns

$$\frac{EI_{effcalc}}{EI_g} = \frac{0.45 + 2.5\eta}{\left[1 + 110\left(\frac{\phi_r}{D}\right)\left(\frac{D}{a}\right)\right]} \leq 1.0 \geq 0.2 \quad 3.15$$

where ϕ_r is the rebar diameter; P is the design normal load; η is the normalized axial stress.

Priestley (1998)

Priestley (1998) demonstrated that flexural stiffness is mostly governed by the axial load ratio and the percentage of steel used.

$$E_c I_e = \frac{M_n}{\phi_y} \quad 3.16$$

where E_c = modulus of elasticity of concrete, M_n = nominal flexural strength of the section and ϕ_y= curvature at first yield. Because ϕ_y is basically a constant for a given f_y, the equation suggests that the flexural rigidity of the member is proportional to its flexural strength. He also said that assuming I_e in a constant proportion of I_g independent of reinforcing content and yield strength is incorrect.

Mirza (1990)

Mirza (1990) examined the parameters influencing the flexural stiffness of slender columns and developed equations taking the eccentricity ratio into account. The stiffness measurements in his investigation were generated using roughly 9500 columns. Following that, the El expressions were statistically created for usage in slender column designs.

$$EI = \left[\left(0.27 + 0.003\frac{l}{h} - 0.3\frac{e}{h}\right)E_c I_g + E_s I_{se}\right] \geq E_s I_{se} \quad 3.17$$

where E_c and E_s are the modulus of elasticity of concrete and steel respectively; I_g is the moment of inertia of gross section and I_{se} is the moment of inertia of steel reinforcement; $E_c I_g$ and $E_s I_{se}$ are the stiffnesses of gross concrete cross-section and steel reinforcement calculated as per the ACI building code; e/h is the end eccentricity ratio.

Kumar and Singh (2010)

Kumar and Singh (2010) published design estimates for the effective stiffness of cracked RC frames made of either normal-strength or high-strength concrete. The parameters that influence the effective stiffness of RC frame members have been established.

For normal strength concrete

For $\eta \leq 0.2$

$$\frac{E_c I_{eff}}{E_c I_g} = 0.35 \quad 3.18$$

For $0.2 \leq \eta \leq 0.6$

$$\frac{E_c I_{eff}}{E_c I_g} = 0.175 + 0.875\eta \quad 3.19$$

For $\eta \geq 0.6$

$$\frac{E_c I_{eff}}{E_c I_g} = 0.7 \quad 3.20$$

For high strength concrete

For $\eta \leq 0.1$

$$\frac{E_c I_{eff}}{E_c I_g} = 0.35 \quad 3.21$$

For $0.1 \leq \eta \leq 0.6$

$$\frac{E_c I_{eff}}{E_c I_g} = 0.24 + 1.1\eta \quad 3.22$$

For $\eta \geq 0.6$

$$\frac{E_c I_{eff}}{E_c I_g} = 0.9 \quad 3.23$$

Where η is the normalized axial stress; EI_{eff} is the effective stiffness and E_c is the elastic modulus of concrete.

Kaushik and Mane (2010)

Kaushik and Mane (2010) suggested a straightforward approach for estimating realistic cracked section characteristics of reinforced concrete columns and beams. His parametric research included around 11,000 beam and column sections. He found that

the effective stiffness of RC beam and column sections was largely determined by the percentage of steel, the axial load ratio, and the eccentricity of the applied axial force.

For $0 \leq \mathrm{ALR} < 0.2$

$$\frac{E_c I_{eff}}{EI_{gross}} = \frac{f_y{}^{0.4} D^{0.07} \rho^{1.2}}{f_{ck}{}^{0.1}} \quad 3.24$$

For $0.2 \leq \mathrm{ALR} \leq 1.8$

$$\frac{E_c I_{eff}}{EI_{gross}} = \frac{f_{ck}{}^{0.2} f_y{}^{0.1} D^{0.2} \rho^{0.5} \mathrm{ALR}^{0.2}}{4.25} - 0.1\mathrm{ALR}^2 \quad 3.25$$

where f_y is the yielding stress of reinforcement bars; ALR refers to the axial load ratio; E_c is the elastic modulus of concrete; D is the diameter of a circular column or the height of a rectangular column.

3.3 Evaluation of Overstrength and Ductility factor

Generally, structures are designed to resist a much higher strength than what is required. It has become a normal practice to provide members with greater sizes and higher material strengths than the minimal design requirements estimated using the design codes. The overstrength factor (Ω) can be defined as the ratio of the first significant yield strength of the structure to the design base shear of the structure.

$$\Omega = \frac{V_y}{V_d} \quad 3.26$$

Ductility is the capacity of a structure to withstand a large deformation without undergoing failure. In structural engineering, the displacement ductility ratio (μ) and ductility reduction factor (R_μ) are widely used to define the ductility of a structure. Furthermore, ductility is often used in earthquake engineering to indicate a structure's capability to sustain massive lateral displacements caused by strong ground motion during an earthquake. The displacement ductility ratio (μ) is the ratio of the system's highest absolute relative displacement to its yield displacement (Miranda, 1993), and it represents the amount of inelastic deformation experienced by the system under a given ground motion.

$$\mu = \frac{\mathrm{Max}|\mu(t)|}{\mu y} \quad 3.27$$

The equation proposed by Miranda and Bertero is:

$$\phi=1+\frac{1}{12\text{T-}\mu\text{T}}-\frac{2}{5T}exp\left[-2\left(lnT-\frac{1}{5}\right)^2\right] \quad 3.28$$

$$R_\mu=\frac{\mu-1}{\phi}+1 \quad 3.29$$

ϕ = function required to calculate approximate strength-reduction factor

T = Period of vibration

3.4 Analysis Procedure

In order to determine the distribution of forces and deformations due to gravity and lateral loads, an analysis of the structure is done such that it addresses the seismic demands and the capacity to resist those demands for all elements in the structure. The most commonly used analysis procedures are described below.

1. Linear Static Analysis: In this method, the forces are based on the code-based fundamental time period of the structure. This method is also commonly known as the Equivalent Static method. The design base shear is calculated for the entire structure and then distributed throughout its height. Based on the floor diaphragm action, the design lateral forces are distributed to the individual lateral load resisting elements.

2. Linear Dynamic Analysis: This method takes the various mode shapes of a building into account. A response is retrieved from the design spectrum for each mode based on the modal frequency and modal mass. The responses are then combined using the absolute sum, square root sum of squares, or complete quadratic combination approach to provide an approximation of the structure's total response. Because the applied loads are considered to be time-dependent, the accelerations and velocities of the excited system are important, thus, inertial and damping forces should be addressed in the formulation.

3. Non-Linear Static Analysis: Non-linear static analysis, often known as pushover analysis, is a tool used to assess the seismic performance of existing or new structures. A nonlinear relationship exists between applied forces and displacements in this type of analysis. This effect can be generated by geometrical nonlinearity as well as material

nonlinearity. The output of this method of analysis is represented in the form of a load versus displacement curve.

4. Non-Linear Dynamic Analysis: This method considers the non-linearity of the structure to analyze the influence of dynamic loading on the structure. It is the most complicated approach of study, attempting to fully reflect the seismic reaction of structures. It is a step-by-step investigation of a structure's dynamic reaction to a specific loading that varies over time.

3.5 Pushover Analysis

Pushover Analysis is a simplified non-linear static analysis procedure that is useful for estimating structural deformations due to seismic forces. The output of this process is represented by a load vs displacement curve. The lateral loads that are applied to the structure approximately represent the seismic forces. The analysis is continued until the failure of the structure occurs, thus, helping to determine the ultimate load at which the collapse occurs as well as its ductility capacity.

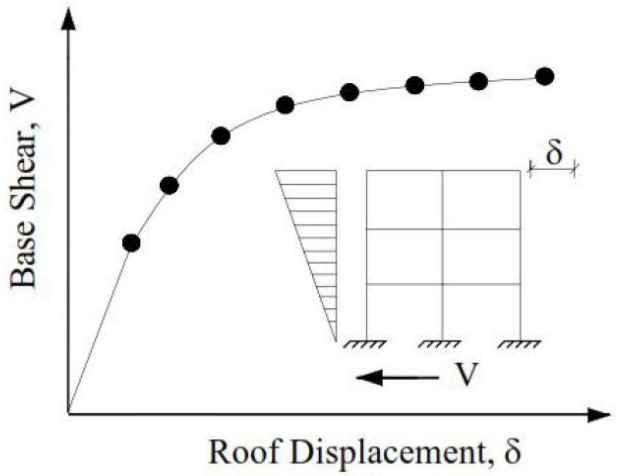

Figure 3-2 Pushover Curve

Figure 3-2 shows a curve plotted between the base shear and the roof displacement which is also known as the Pushover Curve and it provides the key data for determining the overstrength and ductility factors. The structure is subjected to a monotonically increasing lateral force in order to calculate the seismic demand by the nonlinear static procedure. The lateral force is applied until the target displacement value or the ultimate limit state is reached.

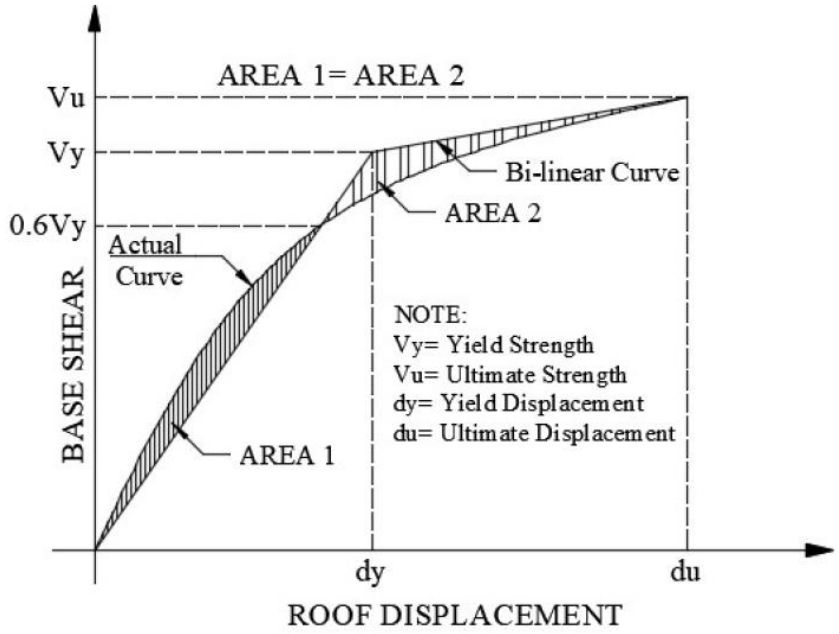

Figure 3-3 Bilinear Idealization of a pushover curve

A bilinear curve as shown in Figure 3-3, represents a plot of two straight lines intersecting at a point (V_y, u_y) which signifies the beginning of non-linearity. This point is also referred to as the yielding point which provides the values of yield displacement as well as yield base shear. According to FEMA 356:2000, “The line segment on the idealized force-displacement curve shall be identified using an iterative graphical approach that approximately balances the area above and below the curve. The effective lateral stiffness, K_e, is defined as the secant stiffness evaluated at a base shear force equal to 60% of the structure's effective yield strength." The following two criteria must be fulfilled.

1. The line segments on the idealized force-displacement curve must be adjusted so that the area above and below the curve is balanced.
2. The first segment of the bilinear curve must intersect the original curve at 60% of significant yield strength.

Force-Displacement Relationship

In non-linear static analysis, the force-displacement relationship of frame elements is frequently represented by the plastic hinges allocated to the desired location of frame elements. Plastic hinges are assigned to those points where the yielding of members is expected. Figure 3-4 shows the force-displacement criteria for hinges as defined in FEMA-356.

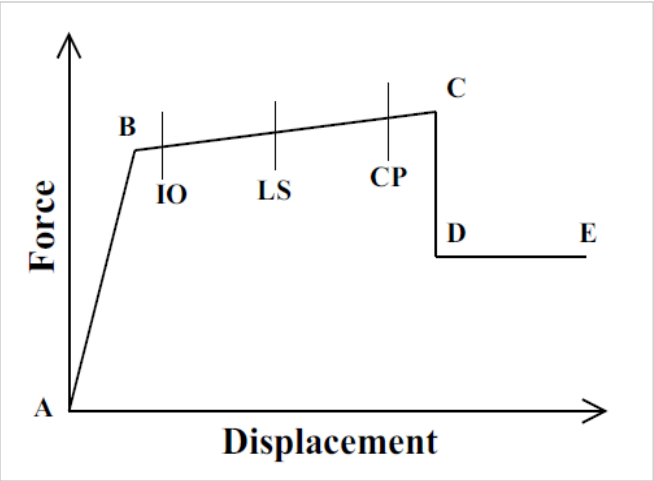

Figure 3-4 Force-Deformation Curve (FEMA 356)

Point A: It indicates the origin and it denotes the unloaded condition.

Point B: It represents yielding. The linear elastic range is represented by AB i.e. A being the unloaded state and B representing the effective yield. No deformation occurs in the hinge up to point B regardless of the deformation value specifies for point B. The slope from B to C portion is very small and represents the strain hardening phenomenon.

Point C: It signifies the ultimate capacity for pushover analysis.

Point D: The residual strength for pushover analysis is denoted by point D where CD shows a sudden reduction in load resistance. The residual resistance from D to E allows the frame elements to sustain gravity loads.

Point E: It denotes the state of complete failure and beyond point E, the hinge will drop the load on the horizontal axis.

The non-linear hinges are categorized by dividing BC into four parts namely, Immediate Occupancy (IO), Life Safety (LS) and Collapse Prevention (CP) which lie within the ductile range BC.

3.6 Fragility Analysis

Vulnerability assessment is required for the identification of the deficiencies in a structure which would eventually facilitate repair and retrofit related tasks. The fragility function can be defined as the conditional probability that the structure will exceed a certain degree of failure due to the seismic forces acting on the structure. It can be used for the evaluation of the seismic performance of a structure. Fragility analysis can also be used to demonstrate the relationship between ground motion severity and the damage state of the structure in a probabilistic manner. The output of fragility analysis can be presented in terms of fragility curves or probability matrices. The fragility curve is defined by a median value of demand parameter i.e., spectral displacement that corresponds to the threshold of the damage state and by the variability associated with that damage state. It represents the probability of exceeding a certain damage state as a function of seismic ground motion. As per the HAZUS methodology, the conditional probability of being in, or exceeding, a particular damage state, given the spectral displacement, S_d is defined by the function:

$$P[ds|S_d] = \phi\left[\frac{1}{\beta_{ds}}\ln\left(\frac{S_d}{\bar{S}_{d,ds}}\right)\right] \quad 3.30$$

Where $\bar{S}_{d,ds}$ is the median value of spectral displacement at which the building reaches the threshold of the damage state.

β_{ds} is the standard deviation of the natural logarithm of spectral displacement for damage state, ds, and ϕ is the standard normal cumulative distribution function.

The scattering of fragility curve for a certain damage state threshold depends on the lognormal variability which is related by the capacity curve $\beta_{c,}$ the lognormal variability related with the demand spectrum β_D, the lognormal variability related through the discrete threshold of individual damage state $\beta_{T,\,ds}$.

$$\beta_{ds} = \sqrt{(\mathrm{CONV}[\beta_c, \beta_d])^2 + \left(\beta_{T,ds}\right)^2} \quad 3.31$$

A convolution procedure is required to check out the overall variability β_{ds} as shown in Equation 3.31. In order to develop the fragility curve, the estimation of variability is a complex numerical method that requires a wide range of statistical data. The variability for the estimation of fragility for low, mid and high-rise buildings has been

provided in HAZUS. The convolution process $\mathrm{CONV}[\beta_c, \beta_d]$ requires a complex mathematical calculation that is very difficult to perform as the demand and capacity is correlated. Hence, the precalculated values of β_{ds} are taken from HAZUS by considering the moderate condition for which the value of β_c=0.3 and $\beta_{T,ds}$=0.4.

Table 3-1 Structural Fragility Curve Parameters for β_{ds}- Moderate Seismic Code

Building Class	Post-yield Degradation of Structural System		
	Structural Systems with Moderate Capacity Variability β_c =0.3		
	Slight	Major	Extreme
	Damage Variability $\beta_{T,ds}$ Moderate (0.4)	Damage Variability $\beta_{T,ds}$ Moderate (0.4)	Damage Variability $\beta_{T,ds}$ Moderate (0.4)
Low-Rise (1-3)	0.80	0.95	1.05
Mid-Rise (4-7)	0.75	0.85	1.00
High-Rise(8-more)	0.70	0.80	1.00

The consideration of damage states is essential for the development of fragility functions. Four damage states are explored in this investigation, as indicated by HAZUS, which are based on structural performances to determine damage state thresholds. The damage state thresholds recommended by Barbat et al. (Table 3-2) which is based on the yield and ultimate spectral displacement has been used. From the bi-linearization of the capacity curve, the value of yield spectral displacement (S_{dy}) and ultimate spectral displacement (S_{du}) are obtained.

Table 3-2 Damage State thresholds (Barbat et al., 2008)

Damage Grade	Damage state	Damage state thresholds
DG1	Slight	$\bar{S}_{d1}$= 0.7 S_{dy}
DG2	Moderate	$\bar{S}_{d2}$= S_{dy}
DG3	Extensive	$\bar{S}_{d3}$=S_{dy}+0.25(S_{du}-S_{dy})
DG4	Complete	$\bar{S}_{d4}$= S_{du}

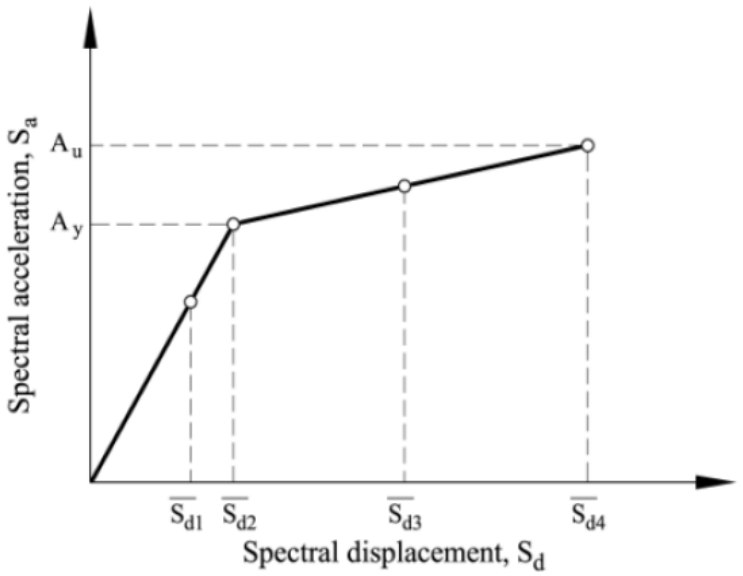

Figure 3-5 Damage State Thresholds (Barbat et al., 2008)

Table 3-3 Probability of Exceedance at different damage states

Damage State	Probability of Exceedance
Complete Damage	P [CD] = P [C | S_d]
Extensive Damage	P [ED] = P [E | S_d] - P [C | S_d]
Moderate Damage	P [MD] = P [M | S_d] - P [E | S_d]
Slight Damage	P [SD] = P [S | S_d] - P [M | S_d]
No Damage	P [None] = 1 - P [S | S_d]

CHAPTER 4: CASE STUDY

4.1 General

The mathematical model of a building structure is a requisite for the design and analysis of the structures. Thus, it is important to develop a mathematical model that closely represents the real structure. To reduce the level of analytical complexity, different assumptions are made while designing and analysis of the structure. In this particular study, ETABSv19 is used for both linear static analysis and design and non-linear static analysis.

4.2 Assumptions and Limitations

With the aim of simplifying the problem with minimum variation in results, the following assumptions were made.

- Infill wall: The stiffness of the infill wall that might affect the overall stiffness of the lateral load resisting system is not considered. However, the mass of the infill wall is applied on the beam as a uniformly distributed load.
- Rigid Foundation: It is assumed that there is no soil-structure interaction i.e., the foundation is assumed to be rigid. However, in reality, the structure always interacts with the soil that causes soil deformation.
- Floor slabs: Floor slabs are assumed to be rigid in their own plane. This assumption reduces the number of unknown displacements to be determined.
- Participating elements: In this study, only the primary components i.e., beam, column and slab are assumed to participate in the response. The effects of secondary structural components and non-structural components are assumed to be negligible.
- Secondary effects like temperature, shrinkage, creep, etc. are not considered.

4.3 Scope of Modeling

Various models with and without the consideration of cracked section properties are modeled for analysis. The buildings with an equal number of bays in both horizontal directions are considered in this study. However, this study is limited to various combinations of buildings with the storey number varying from 2 to 6, the bay number varying from 2 to 5, the bay length of 3.5m with the storey height of 3m.

4.4 Building Nomenclature

The varying parameters considered in this study are the number of storeys, number of bays, gross section and cracked section. mS and nB represents the building having m number of storey and n number of bay and the terms G and C are used to denote gross and cracked section respectively. For instance, 4S4BG denotes a building having 4 storeys and 4 bays modeled using gross section and 4S4BC denotes a building having 4 storeys and 4 bays modeled using cracked section

4.5 Material Properties and Sections

The concrete grade used is M25 with an elastic modulus equal to 25000 MPa with Poisson's ratio of 0.2. Reinforcement grade HYSD500 TMT with an elastic modulus of 200000 MPa and Poisson's ratio of 0.3 is used in the design process.

The slab is defined as an area section of thickness 125mm. The column and beam size adopted for different buildings are listed in the table below.

Table 4-1 Column and beam size adopted for different models

No. of storey	Beam size (mm × mm)	Column size (mm × mm)
2	250 × 300	300 × 300
3	250 × 300	350 × 350
4	300 × 400	400 × 400
5	300 × 400	400 × 400
6	300 × 400	450 × 450

4.6 Loads and Load Combination

Following loads have been included in the calculation.

1. Dead Load
2. Live load of 3 KN/m^2 on all floors and 1.5 KN/m^2 on the roof.
3. Floor finish of 1 KN/m^2 on all slab
4. Lateral Load
5. Wall load as uniformly distributed load on beams.
   Wall load for external wall = 8.57 KN/m
   Wall load for internal wall = 5.71 KN/m
   Parapet wall load = 3.67 KN/m

Seismic Weight

The total seismic weight of the structure, W, shall be taken as the sum of the dead loads and factored seismic live loads, i.e.

$$W = DL + \lambda LL \qquad 4.1$$

Where, W is the total seismic weight of the structure,

DL is the total dead load of the structure which includes the self-weight of the structural elements, floor finish and wall loads

LL is the live load and λ is the live load participation factor. It is taken as 0.30 in this study.

Horizontal Base Shear Coefficient

Ultimate Limit State	**Serviceability Limit State**
$C_d(T_1) = \frac{C(T_1)}{R_\mu \times \Omega_u}$ Where, $C(T_1)$ is the Elastic Site Spectra R_μ is the Ductility factor (taken as 4 in this study) Ω_u is the Overstrength Factor for Ultimate Limit State (taken as 1.5 for this study)	$C_d(T_1) = \frac{C_s(T_1)}{\Omega_s}$ Where, $C_s(T_1)$is the Elastic Site Spectra for Serviceability Limit State Ω_s is the Overstrength Factor for Serviceability Limit State (taken as 1.25 for this study)

The Elastic Site Spectra for horizontal loading shall be as given by the equation below:

$$C(T) = C_h(T)ZI \qquad 4.2$$

Where,

Ch(T) is the Spectral Shape factor

Z is the Seismic Zoning factor (taken as 0.35 for this study)

I= Importance factor (taken as 1 for this study)

Load Combination

For the design of a structure, the seismic load effect is combined with other effects. The following combination is adopted to design the structure.

1.2DL+ 1.5LL

DL+ λLL+ E

DL+ λLL- E

Where λ is 0.6 for storage facilities, 0.3 for other usages and nil for the roof.

Seismic Loading

Seismic loads for selected building models were computed in accordance with NBC 105:2020. The equivalent static method was used to compute the base shear coefficient. The step-by-step technique for calculating the seismic load and distributing it among different floors as specified in NBC 105:2020 has been elaborated below.

Step 1: Calculation of seismic weight (Wi)

The seismic weight (Wi) at each level is the summation of the dead loads (DL) and factored live load (LL) between the mid heights of adjacent stories.

$$W_i = DL + \lambda LL \qquad 4.3$$

Where λ is 0.6 for storage facilities, 0.3 for other usages and nil for the roof.

Step 2: Calculation of fundamental translation period (T)

The fundamental translation period is calculated using the empirical method (Equation 4.4) and the Rayleigh method (Equation 4.5). The value of the period using the empirical equation is increased by a factor of 1.25. The smaller of the two shall be considered for design action.

$$T = K_t H^{3/4} \qquad 4.4$$

Where, K_t = 0.075 for moment resisting concrete frame, and H= height of the building.

$$T = 2\pi \sqrt{\frac{\sum_i^n W_i d_i^2}{g \sum_i^n F_i d_i}} \qquad 4.5$$

Where, W_i= seismic weight, d_i= elastic horizontal displacement of the center of mass, F_i= lateral force acting at i level, g= acceleration due to gravity, i= level under consideration and n= number of levels in the structure.

Step 3: Calculation of spectral shape factor

The spectral shape factor, $C_h(T)$ is obtained from Figure 4-1 corresponding to the fundamental translation period in Step 2. Soil type B was used in this study.

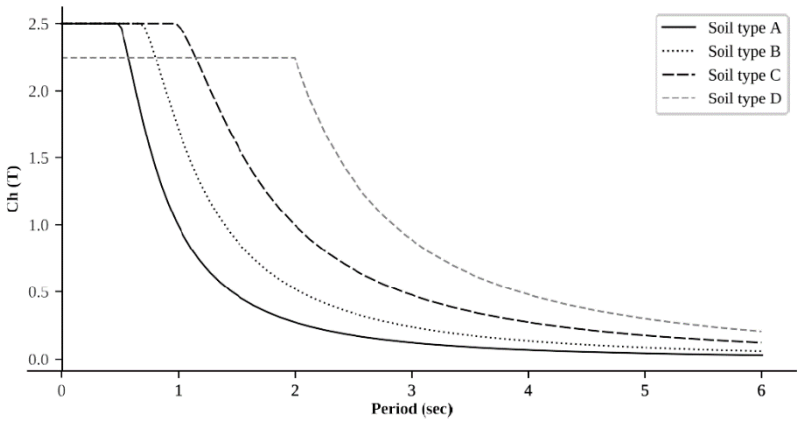

Figure 4-1 Spectral Shape Factor, Ch(T) for Equivalent Static Method (NBC 105:2020)

Step 4: Calculation of elastic site spectra

The elastic site spectra for the ultimate limit state is calculated using Equation 4.6 while

elastic site spectra for serviceability limit state is calculated using Equation 4.7.

$$C_u(T) = C_h Z I \qquad 4.6$$

$$C_s(T) = 0.2 C_u(T) \qquad 4.7$$

where, Z is the seismic zone factor and I is the Importance factor

Step 5: Calculation of horizontal base shear coefficient

The base shear coefficient ($C_{d,u}$) for the ultimate limit state is calculated using Equation 4.8 and the base shear coefficient ($C_{d,s}$) for the serviceability limit state is calculated using Equation 4.9.

$$C_{d,u}(T_1) = \frac{C(T_1)}{R_\mu \times \Omega_u} \qquad 4.8$$

$$C_{d,s}(T_1) = \frac{C_s(T_1)}{\Omega_s} \qquad 4.9$$

Where,

R_μ is the Ductility factor (taken as 4 for this study)

Ω_u is the Overstrength Factor for Ultimate Limit State (taken as 1.5 for this study)

Ω_s is the Overstrength Factor for Serviceability Limit State (taken as 1.25 for this study)

Step 6: Calculation of horizontal seismic base shear

The horizontal base shear (V_u) for the ultimate limit state is calculated using Equation 4.10. For design action of the structure base shear for the ultimate limit state shall be used, and for performance check, both limit state lateral loading shall be used.

$$V_u = C_{d,u} W \qquad 4.10$$

Step 7: Vertical distribution of shear forces

The horizontal seismic base shear is distributed at each floor level (Fi) using the relation given in Equation 4.11.

$$F_i = \frac{W_i h_i^k}{\sum_i^n W_i \, h_i^k} \times V \qquad 4.11$$

Where, W_i= Seismic weight at i^{th} level

h= height from base to level i

K= 1 for $T \leq 0.5$ sec, 2 for $T \geq 2.5$ sec and for an intermediate value of T linear interpolation between 1 and 2.

Performance Check

The ultimate limit state is based on seismic ground motions with a return period of 475 years. The drift value for the ultimate limit state is calculated by multiplying the horizontal deflection found from the equivalent static method or response spectrum method for the ultimate limit state loading condition with the Ductility factor (R_μ). In the same manner, the drift value for serviceability limit state is obtained by taking the deflection found from the equivalent static method or response spectrum method for serviceability limit state loading condition.

Table 4-2 Performance requirement (NBC 105:2020)

Performance Limit State	Inter-storey Drift Limitation
Ultimate Limit State (ULS)	0.025
Serviceability Limit State (SLS)	0.006

CHAPTER 5: RESULTS AND DISCUSSIONS

5.1 Sample Calculation

The building taken for calculation is of 4 storey and 4 bays, regular in both axes and it is designed as per NBC 105:2020. The building is designated as 4S4BG for building modeled using gross or uncracked section and 4S4BC for building modeled using cracked section. The finite element modeling of the building is done using ETABSv19. Design base shear and fundamental time period of the building is obtained and the designed building is checked to see if all the members are capable of resisting the applied load.

Material non-linearities are assumed by defining frame hinge properties, which represent post-yield behavior. Hinges are placed at the ends of the beam and column where the mechanism is expected. The default hinge is defined for both the beam and the column member. To capture linked axial and biaxial bending behavior, an auto P-M2-M3 hinge is defined for the column. Axial load effects are neglected for beam members due to the rigid floor diaphragm effect, and an uncoupled moment M3 hinge is provided. A pushover curve is obtained which is then converted to get an idealized bilinear plot by equal area approximation. The 3D model of a 4 storey 4 bays model with detailed calculation is presented below.

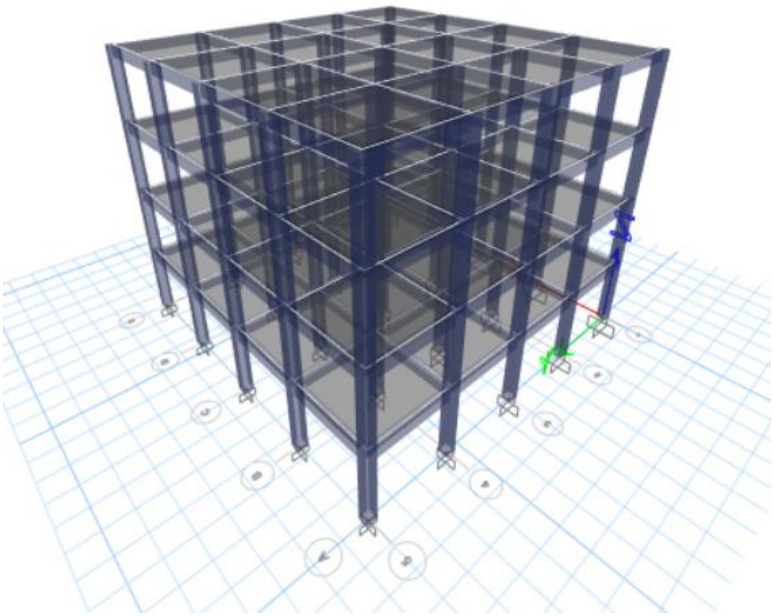

Figure 5-1 Finite Element Modeling of a building model

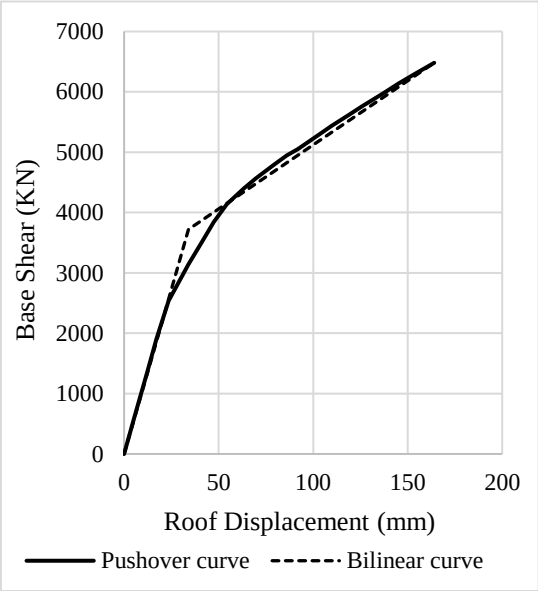

Figure 5-2 Pushover curve and Idealized Bilinear curve for Gross section model. (4S4BG)

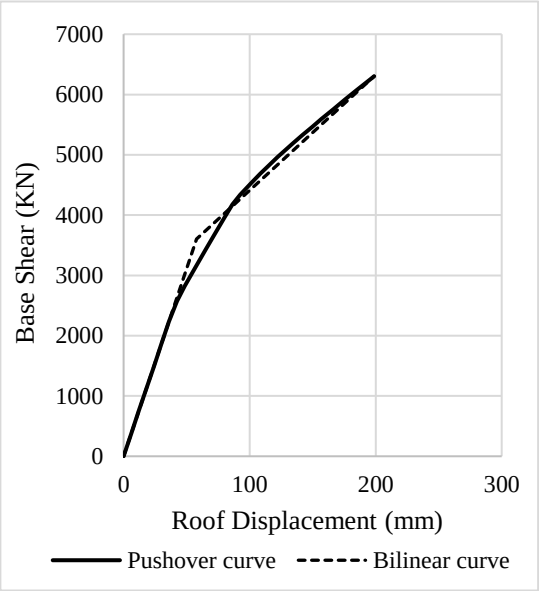

Figure 5-3 Pushover curve & Idealized Bilinear curve for Cracked section model. (4S4BC)

Fundamental Time Period, T= 0.524	Fundamental Time Period, T= 0.698
Yield Strength, V_y = 3721.25	Yield Strength, V_y = 3602.372
Design Base Shear, V_d = 1368.48	Design Base Shear, V_d = 1368.48
Yield Displacement, d_y = 34.064	Yield Displacement, d_y = 57.978
Ultimate Displacement, d_u= 164.047	Ultimate Displacement, d_u= 198.78
Displacement Ductility Ratio, μ= 4.815	Displacement Ductility Ratio, μ= 3.428
Ductility Factor, R_μ = 4.522	Ductility Factor, R_μ = 3.821
Overstrength Factor, Ω = 2.71	Overstrength Factor, Ω = 2.63

The continuous curve represents the pushover curve whereas the dashed line represents the bilinear curve.

Model considering gross section:

$$\Omega = \frac{V_y}{V_d} = \frac{3721.25}{1368.48} = 2.71$$

Model considering cracked section:

$$\Omega = \frac{V_y}{V_d} = \frac{3602.372}{1368.48} = 2.63$$

The ductility reduction factor is calculated by using the expression proposed by (Miranda & Bertero,1994) with respect to ϕ coefficient for alluvium sites.

Model considering gross section:

$$\mu = \frac{du}{dy} = \frac{164.047}{34.064} = 4.815$$

$$\phi = 1 + \frac{1}{12T - \mu T} - \frac{2}{5T} exp\left[-2\left(lnT - \frac{1}{5}\right)^2\right] = 1.083$$

$$R_\mu = \frac{\mu - 1}{\phi} + 1 = 4.522$$

Model considering cracked section:

$$\mu = \frac{du}{dy} = \frac{198.78}{57.978} = 3.428$$

$$\phi = 1 + \frac{1}{12T - \mu T} - \frac{2}{5T} exp\left[-2\left(lnT - \frac{1}{5}\right)^2\right] = 0.860$$

$$R_\mu = \frac{\mu - 1}{\phi} + 1 = 3.821$$

5.2 Effect on Inter-storey Drift

The inter-storey drift was studied by analyzing the models by using gross section and cracked section for analysis and also by varying the number of storeys and number of bays. Each of the following graphs presents the inter-storey drift with respect to gross and cracked section for both ultimate limit state as well as serviceability limit state.

It is observed that the inter-storey drifts of the buildings with uncracked section is less than the cracked section. Due to the reduced stiffness, the structure will be relatively flexible which results in increment in the inter-storey drift in the buildings designed using cracked section.

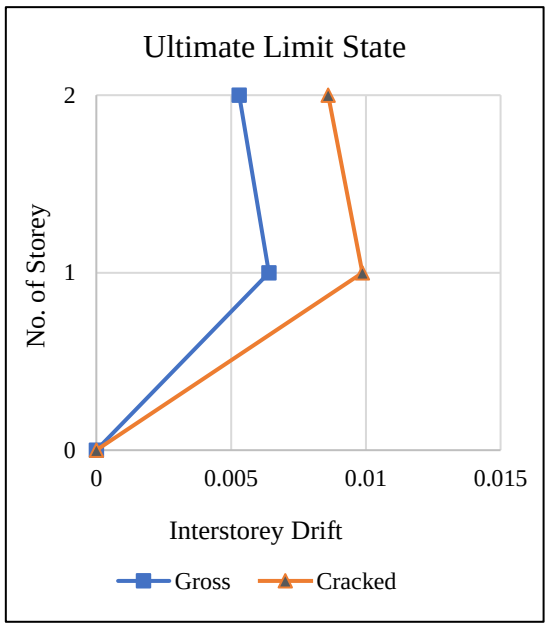

Figure 5-4 Inter-storey drift for 2 storey model (ULS)

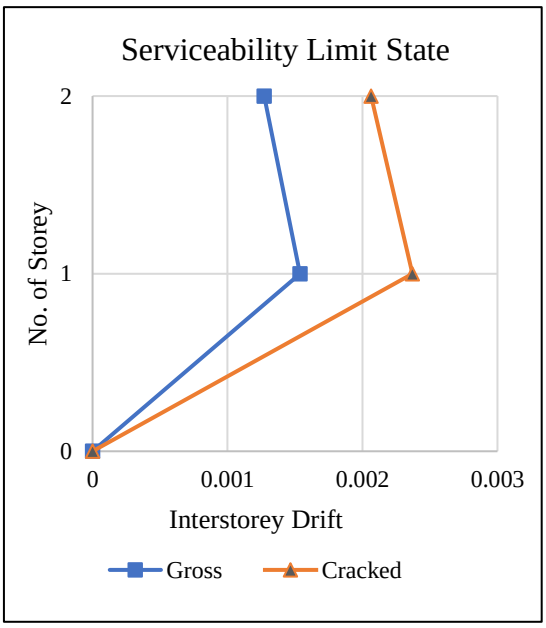

Figure 5-5 Inter-storey drift for 2 storey model (SLS)

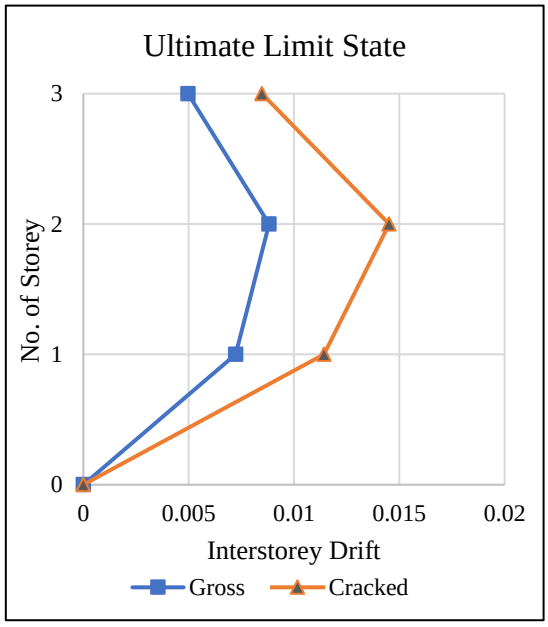

Figure 5-6 Inter-storey drift for 3 storey model (ULS)

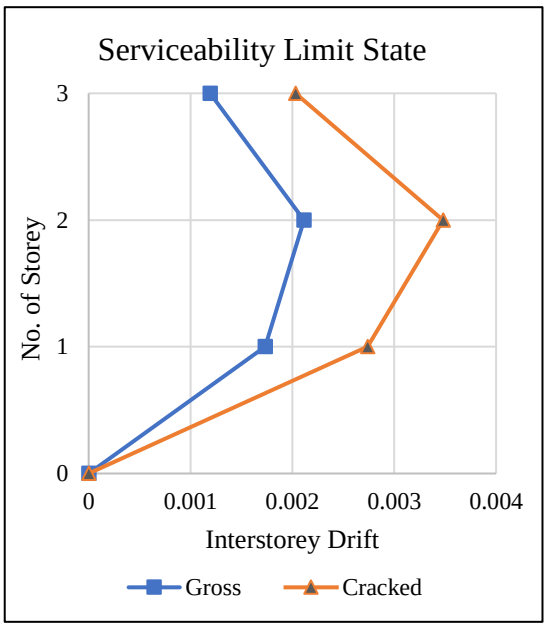

Figure 5-7 Inter-storey drift for 3 storey model (SLS)

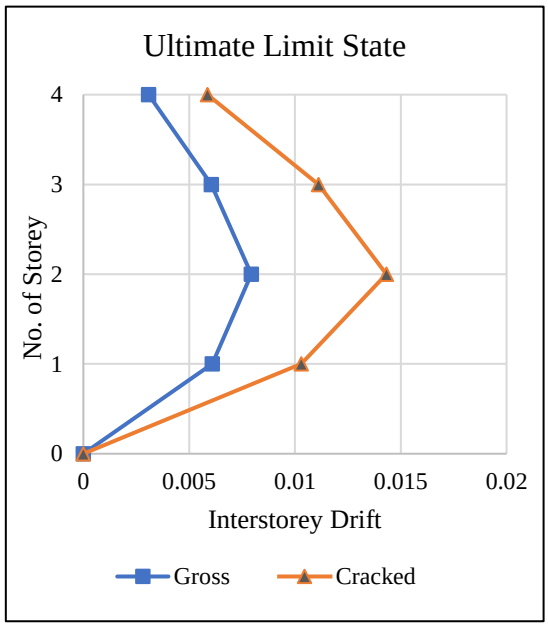

Figure 5-8 Inter-storey drift for 4 storey model (ULS)

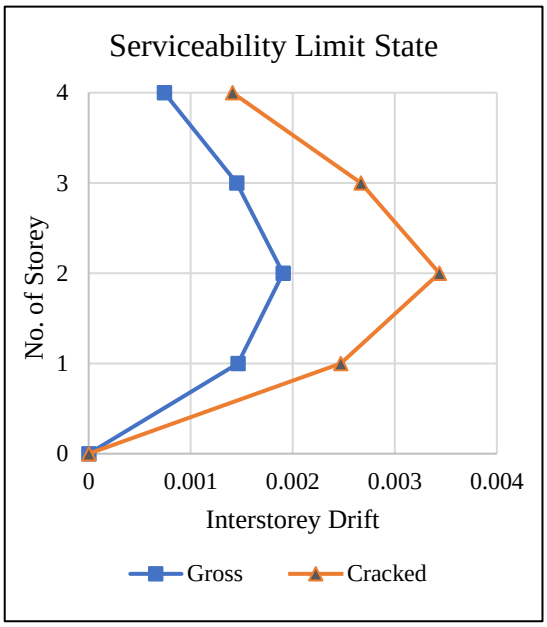

Figure 5-9 Inter-storey drift for 4 storey model (SLS)

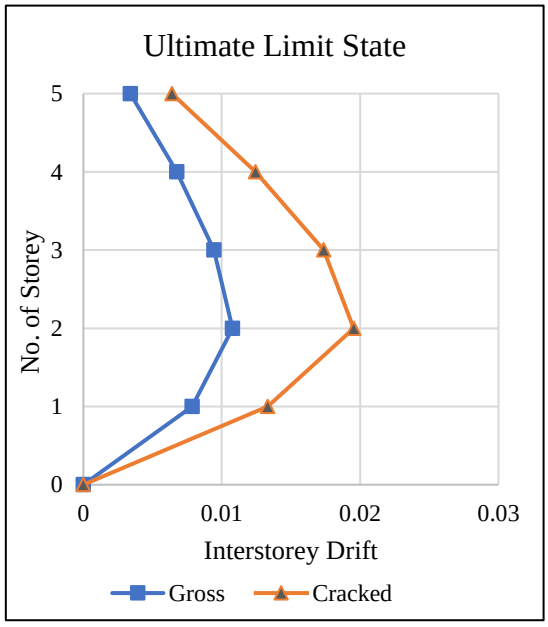

Figure 5-10 Inter-storey drift for 5 storey model (ULS)

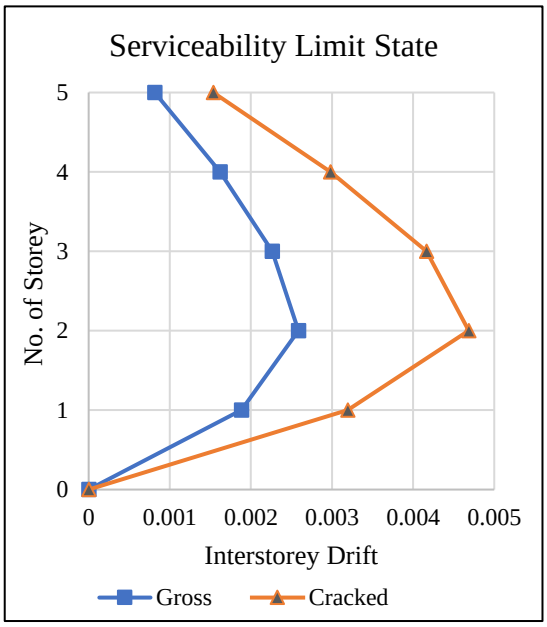

Figure 5-11 Inter-storey drift for 5 storey model (SLS)

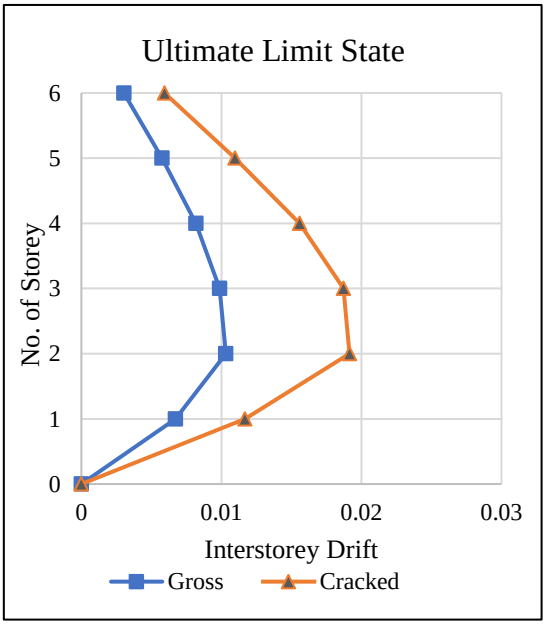

Figure 5-12 Inter-storey drift for 6 storey model (ULS)

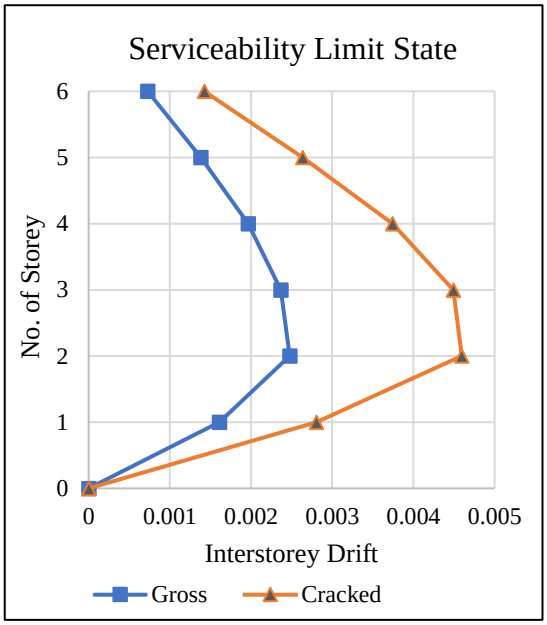

Figure 5-13 Inter-storey drift for 6 storey model (SLS)

5.3 Effect on Time period

For capturing the dynamic properties of a building, proper assessment of the flexural stiffness of individual members is essential. The first mode time period was studied by analyzing the models by using gross section and cracked section. The results indicated that the first mode time period of a building calculated using gross stiffness is lower than the first mode time period calculated using effective stiffness. This can be justified by the fact that stiffer buildings have less time period. While reducing stiffness, the mass is also reduced, thus, during the calculation of the natural period, the mass and stiffness compete to decide whether the natural period will increase or decrease when both are modified.

From Figure 5-14, it is evident that the time period for the cracked section increases as compared to the gross section when the number of storeys is varied. However, the increment in the time period due to an increase in the number of bays is very minimal. The variation in first mode time period for the buildings designed using gross and cracked sections with variation in number of storey and number of bays has been shown in Figure 5-14 and Figure 5-15.

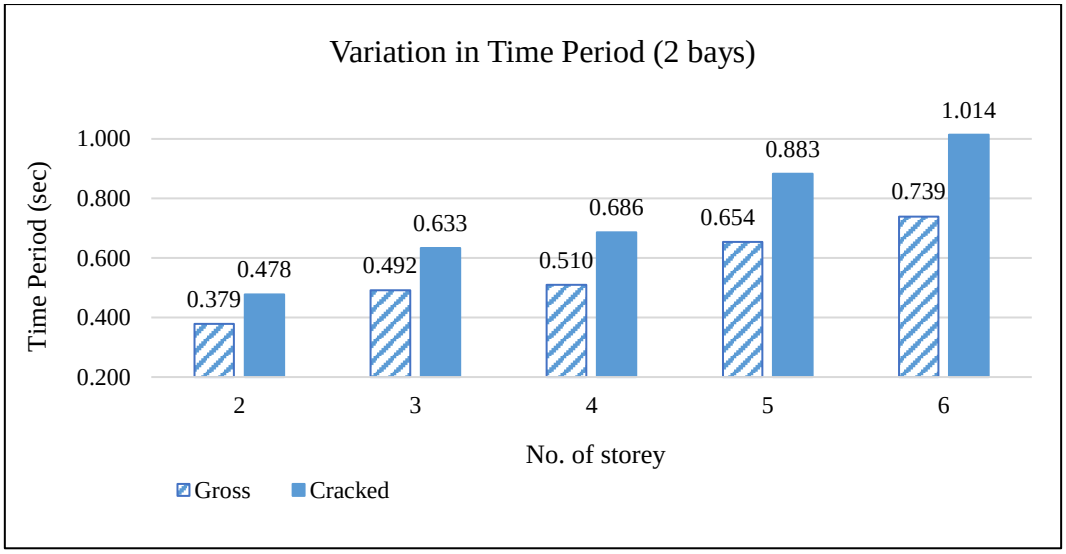

Figure 5-14 Variation in Time period

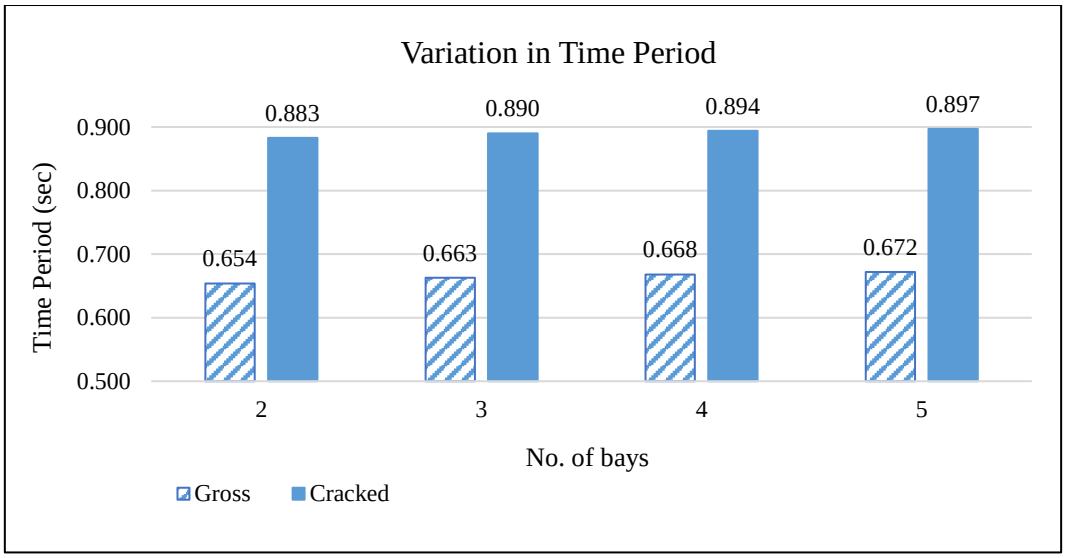

Figure 5-15 Variation in time period for 5-storey model

The change in time period for all the models used in this research has been summarized in the table below.

Table 5-1 Increase in Time Period

No. of Storey	Average increase in time period (%)
2	25.42
3	27.65
4	33.61
5	34.14
6	36.45

5.4 Effect on Overstrength factor

The overstrength factor was studied by analyzing the models by using gross section and cracked section for analysis and also by varying the number of storey and number of bays. Each of the following graphs presents the overstrength factor of the gross section model and cracked section model with variation in the number of storey and number of bays.

The overstrength factor for buildings using gross section was found to be higher than that of cracked section even though it was by a slight margin. The overstrength factor is determined by the yield base shear and the design base shear, but the value of the design base shear was the same in both cases. As the value of the yield base shear for the gross section model was found to be more than the cracked section, the overstrength factor for the gross section was found to be higher.

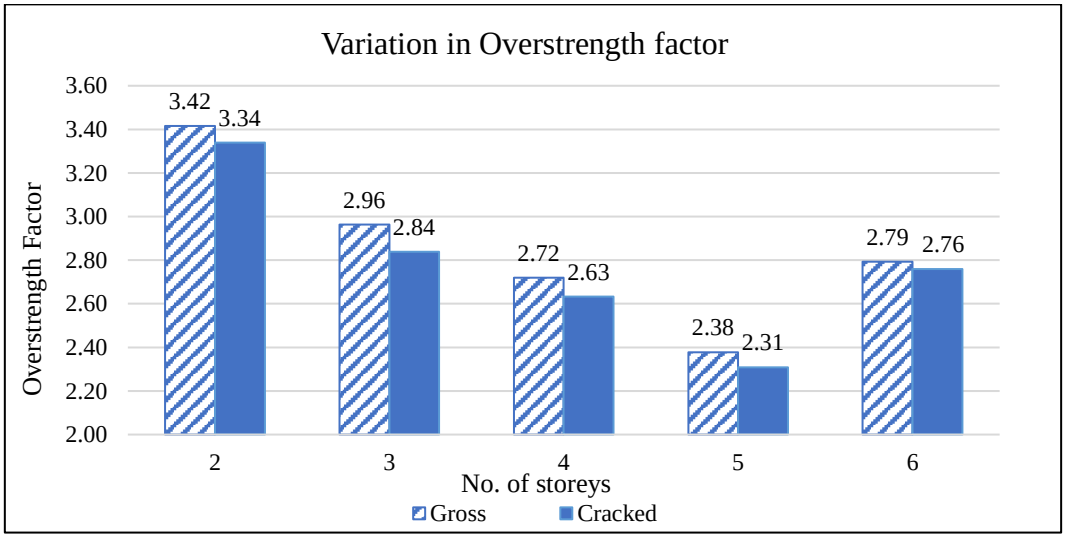

Figure 5-16 Variation in overstrength factor with increase in no. of storeys (4 bays)

From Figure 5-16, it can be observed that the overstrength factor decreases as the number of storeys increases up to 5 storeys for both gross and cracked section. However, it is evident from the graph that the overstrength factor of 6 storey building is higher than the overstrength factor of 5 storey building. This may be attributed to the fact that overstrength depends upon the yield base shear and the design base shear. An increment in the overstrength factor can be noticed when the yield base shear increases or the design base shear decreases.

In this case, the increase in overstrength factor might be primarily due to the decrease in the value of the seismic base shear coefficient as we ascend from 5 to 6 number of

storeys. This reduction in base shear coefficient ultimately results in the decrease in design base shear value in the case of 6 storey building.

Table 5-2 Overstrength factor for varying number of storeys (4 bays)

No. of storey	Analysis Case	Design Base Shear, V_d (KN)	Yield Base Shear, V_y (KN)	Overstrength factor (Ω)
2	Gross	563.87	1926.06	3.416
	Cracked	563.87	1882.97	3.339
3	Gross	903.01	2675.4	2.963
	Cracked	903.01	2563.34	2.839
4	Gross	1368.49	3721.26	2.719
	Cracked	1368.49	3602.37	2.632
5	Gross	1733.6	4122.21	2.378
	Cracked	1733.6	4001.81	2.308
6	Gross	1944.21	5429.17	2.792
	Cracked	1944.21	5365.19	2.760

From Table 5-2, it can be observed that while increasing the number of storeys, both the design base shear and the yield base shear increase but the yield base shear increases at a lower rate than the design base shear which eventually decreases the overstrength factor.

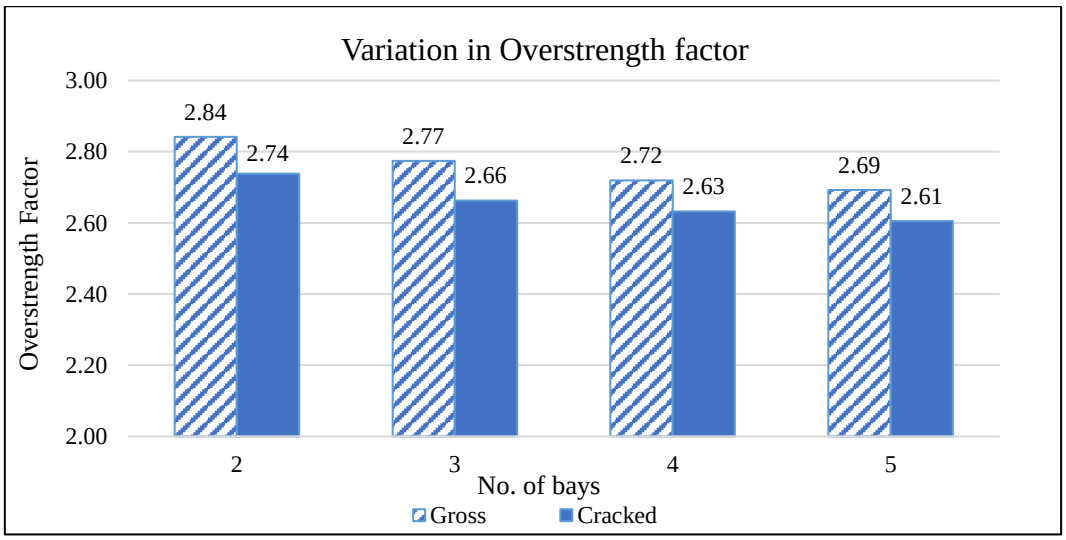

Figure 5-17 Variation in overstrength factor for increase in no. of bays (4 storey)

From Figure 5-17, the effect of the number of bays on the overstrength factor can be observed. Even though the graph shows a decreasing pattern in overstrength factor with the increase in the number of bays, the change is very minor. This may be attributed to the fact that with the increment in the number of bays, the value of both design base

shear and yield base shear increases proportionately such that the overall overstrength factor doesn't differ much.

5.5 Effect on Ductility factor

Likewise, the ductility factor was studied by analyzing the models using gross section and cracked section analysis, as well as by altering the number of storeys and bays. Each of the graphs below depicts the ductility factor of a gross section model and a cracked section model with variations in the number of storeys and bays.

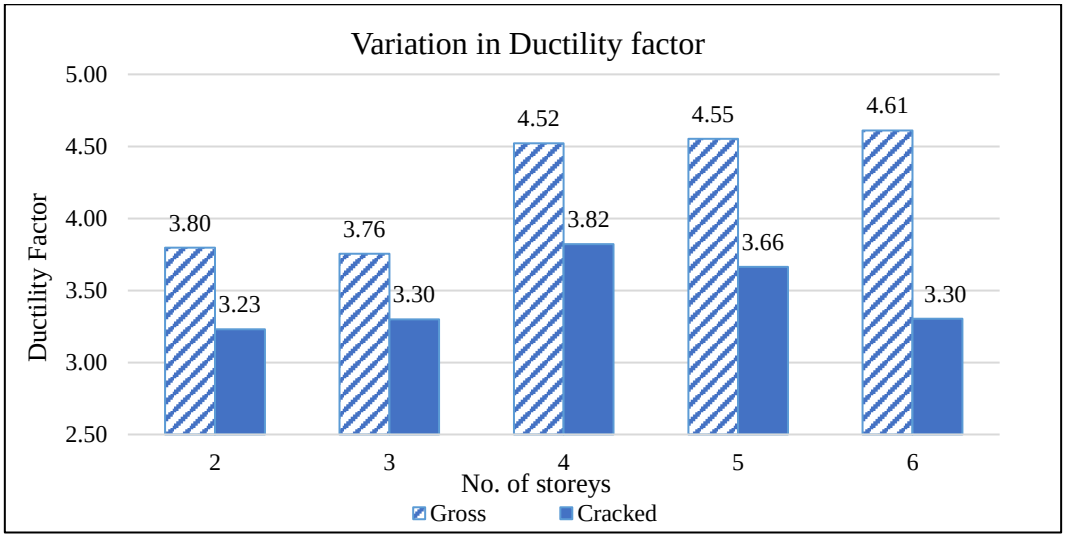

Figure 5-18 Variation in ductility factor with increase in no. of storeys (4 bays)

From Figure 5-18 and Figure 5-19, it can be observed that unlike the overstrength factor, the ductility factor does not follow a specific trend of data variation for different storied building which seems to be consistent with past research (Rajbhandari, 2019).

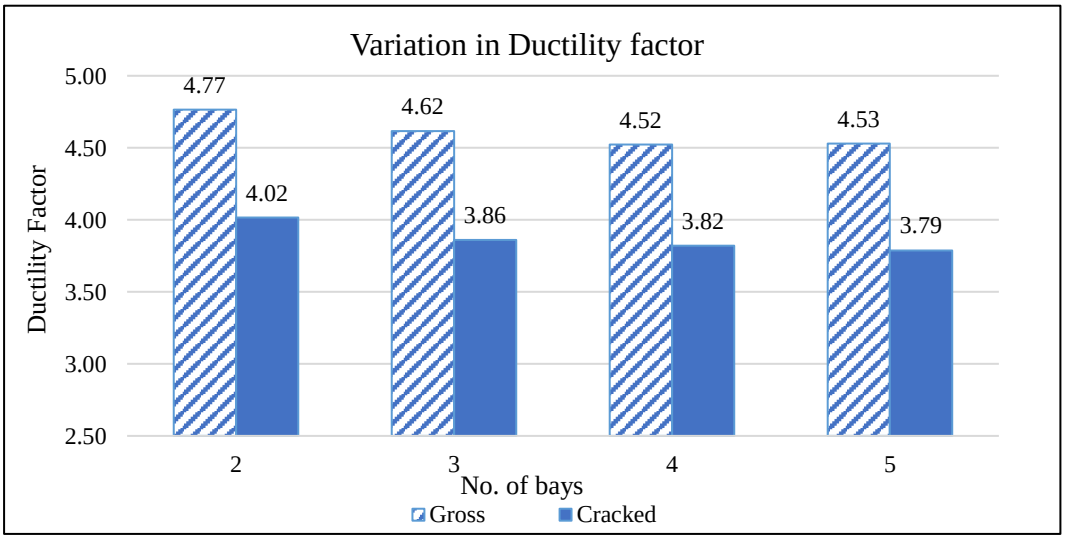

Figure 5-19 Variation in ductility factor with increase in no. of bays (4 storey)

The value of displacement ductility (μ) was found to be larger for the gross section model as compared to the cracked section model. The value of ductility coefficient can also be used to express the inelastic deformation capacity of the structures. The higher the value of this coefficient, the greater the energy absorption and the formation of plastic joints (Monavari and Massumi, 2012).

Table 5-3 Estimation of yield and ultimate displacement

No. of storey	Gross			Cracked		
	d_u	d_y	μ	d_u	d_y	μ
2	106.62	23.68	4.50	123.33	36.40	3.39
3	137.84	34.69	3.97	165.06	53.76	3.07
4	164.05	34.06	4.82	198.78	57.97	3.43
5	201.66	47.91	4.21	248.71	82.49	3.01
6	252.76	62.72	4.03	308.98	114.41	2.70

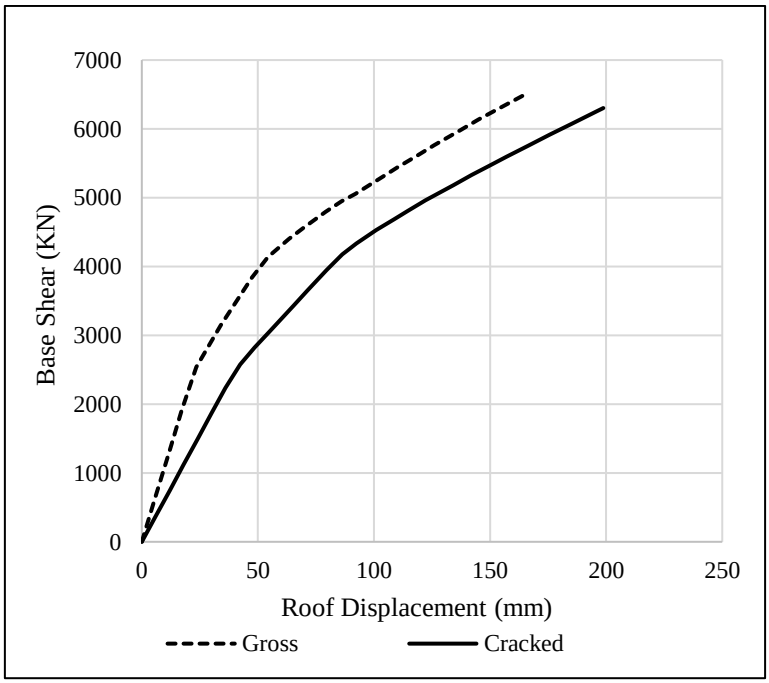

Figure 5-20 Capacity curve for gross and cracked section models

From the capacity curve, it is quite obvious that the ultimate capacity of the cracked section model is less than the gross section model. The obtained values for ultimate displacement also show the effect of reduced stiffness of the cracked section model. Apart from that, there is a considerable difference in the significant yield point. The building designed using a cracked section seems to absorb the same load through the initiation of global or roof displacement whereas the building designed using gross

section resists it by having a higher initial stiffness, which tends to allow less displacement. From the pushover results, it can also be noted that the building designed using gross section overestimates the capacity of the building in terms of base shear.

5.6 Fragility Analysis

Fragility analysis was carried out for the buildings designed using gross as well as cracked section. The fragility curves were developed using HAZUS methodology which is basically a graphical representation to assess the vulnerability of the buildings. The cumulative probability of various damage states is plotted with respect to the spectral displacement representing the intensity measure (IM).

As the consideration of every data is a bit tedious, the results obtained from the fragility analysis of a representative set of buildings are discussed. The buildings chosen for this purpose have 5 number of bays in both direction with variation in number of storeys ranging from 2 to 6.

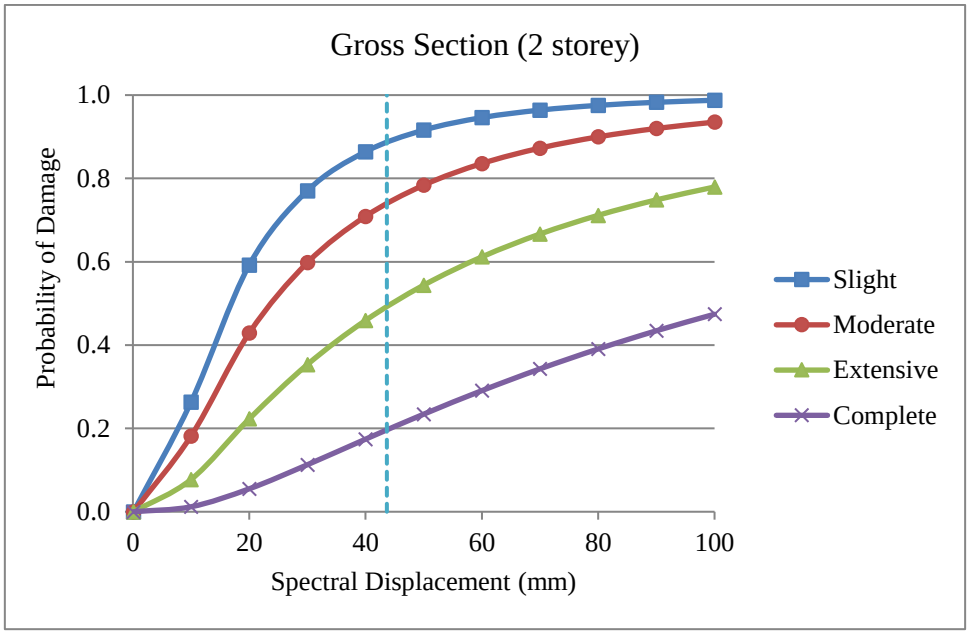

Figure 5-21 Fragility Curve for 2-storey model (Gross)

From Figure 5-21, it is obvious that as the spectral displacement increases, the probability of damage also increases. It also reflects that the probability of slight damage is always the highest and that of the complete damage state is the least. The probability of damage for gross section model having 2 storeys was found to be 88.32%, 73.64%, 49.02% and 19.62% for slight, moderate, extensive and complete damage state respectively.

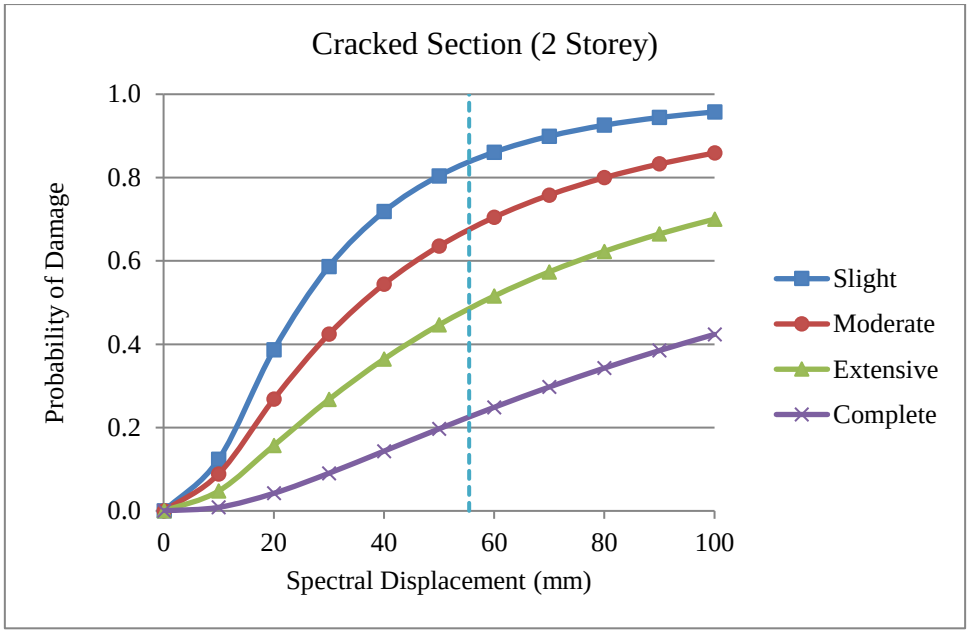

Figure 5-22 Fragility Curve for 2-storey model (Cracked)

Similarly, for a 2-storey building designed using cracked section the probability of damage was found to be 83.52%, 67.32%, 48.42% and 22.52% for slight, moderate, extensive and complete damage state respectively as shown in Figure 5-22.

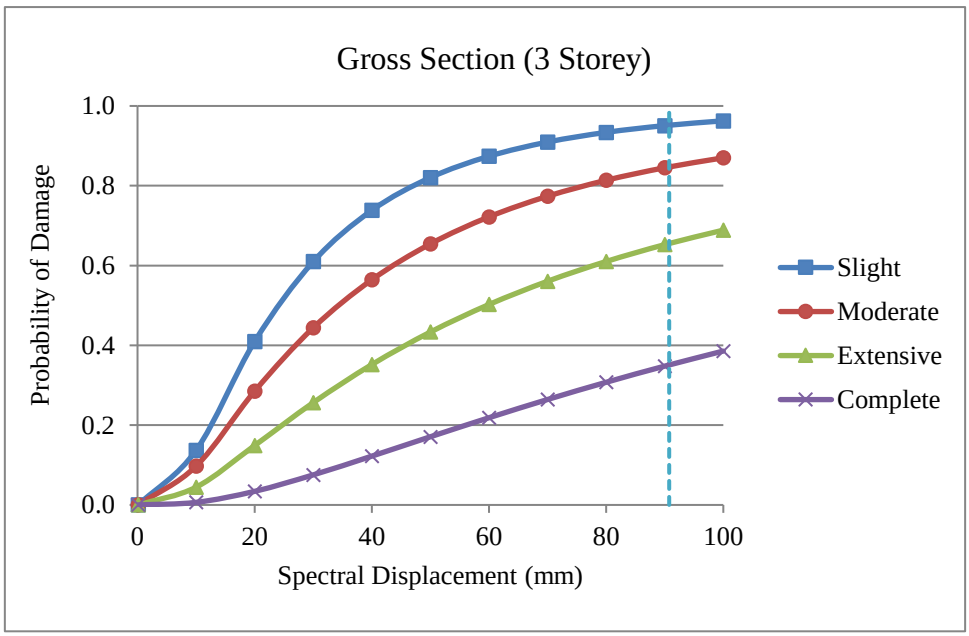

Figure 5-23 Fragility Curve for 3-storey model (Gross)

From Figure 5-23 it can be observed that there is 95.16% chance of experiencing slight damage, 84.7% chance of experiencing moderate damage, 65.5% chance of experiencing extensive damage whereas complete damage has 35.08% chance of occurrence for a 3-storey building designed using gross section.

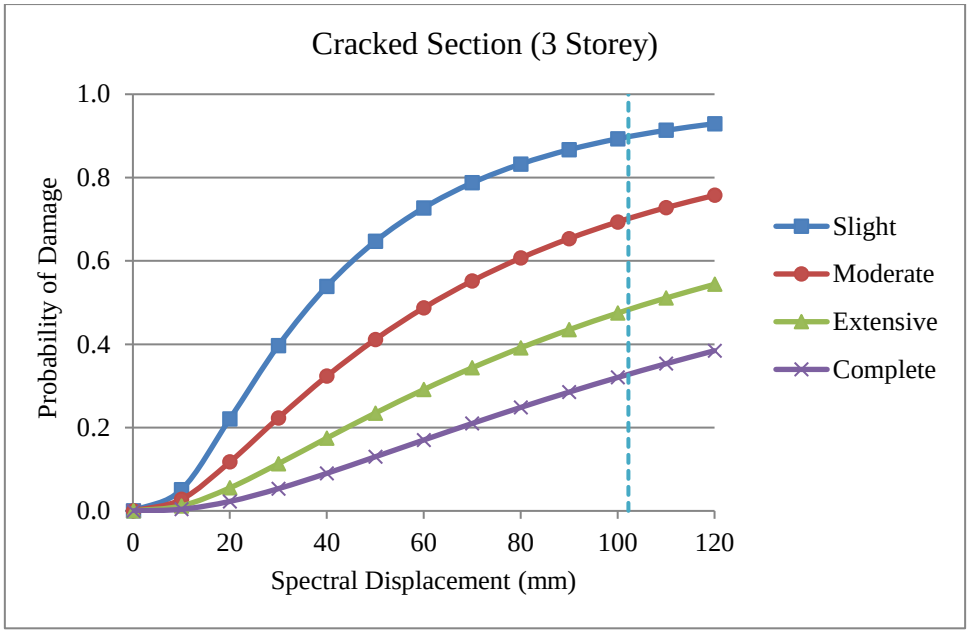

Figure 5-24 Fragility Curve for 3-storey model (Cracked)

Likewise, the probability of damage for cracked section model having 3 storeys was found to be 89.76%,70.12%, 48.28% and 32.75% for slight, moderate, extensive and complete damage state respectively as shown in Figure 5-24.

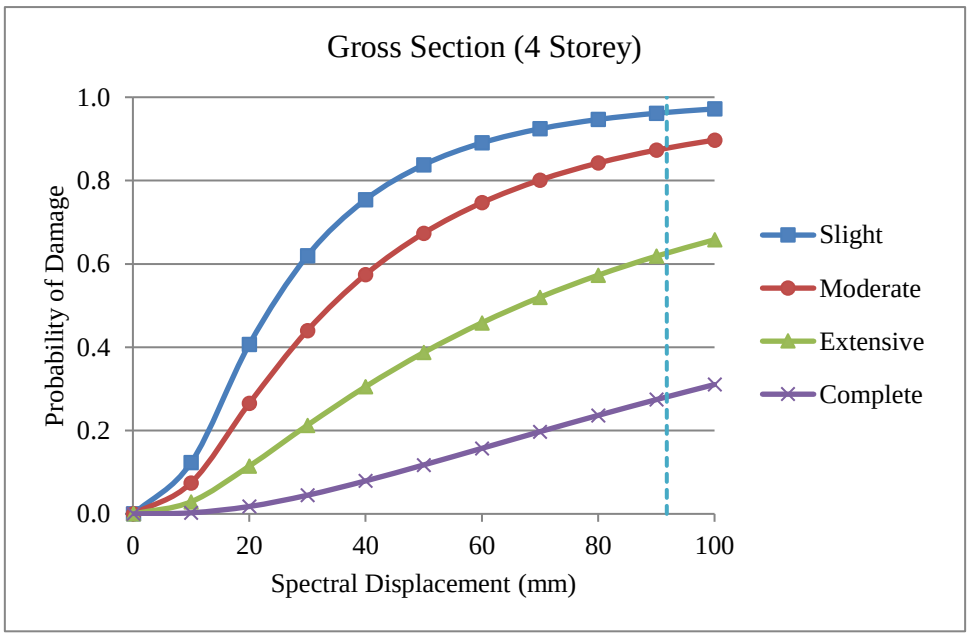

Figure 5-25 Fragility Curve for 4-storey model (Gross)

For a 4-storey building designed using gross section, the probability of damage was found to be 95.51%,85.96%, 60.93% and 27.26% for slight, moderate, extensive and complete damage state respectively as shown in Figure 5-25.

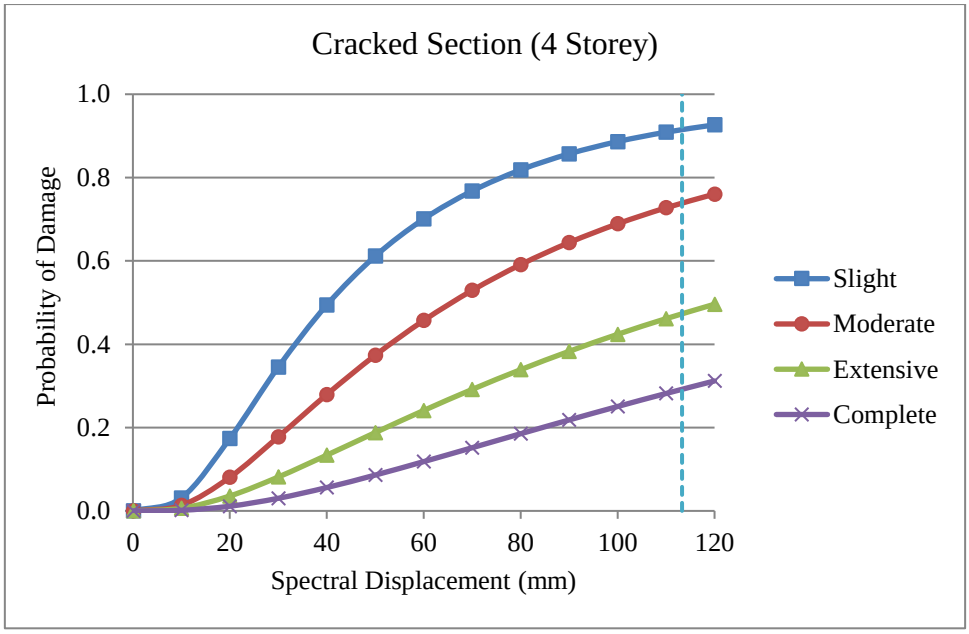

Figure 5-26 Fragility Curve for 4-storey model (Cracked)

Similarly, the probability of damage for cracked section model having 4 storeys was found to be 91.04%,73.83%, 47.28% and 29.17% for slight, moderate, extensive and complete damage state respectively as shown in Figure 5-26.

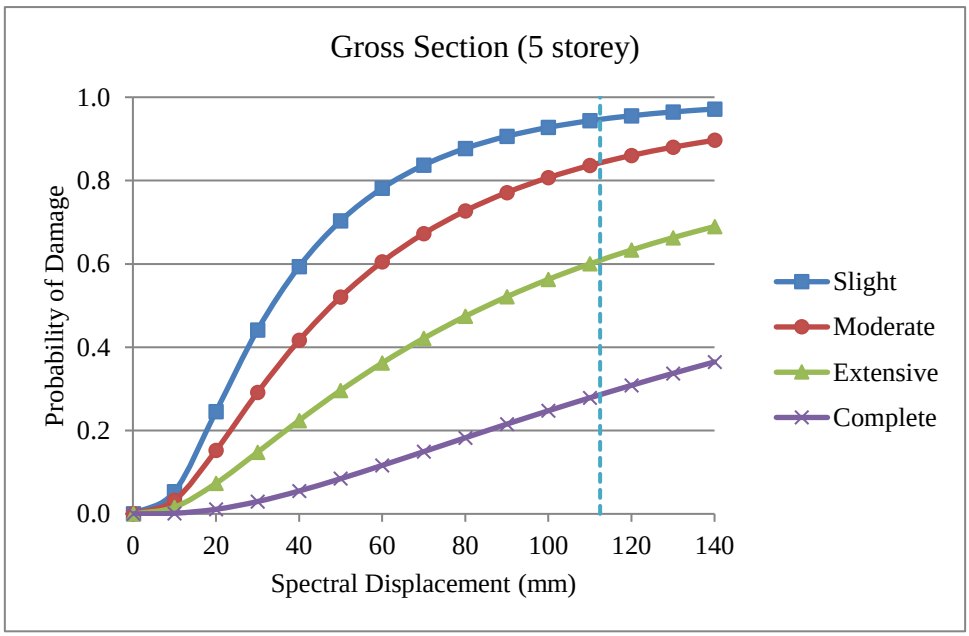

Figure 5-27 Fragility Curve for 5-storey model (Gross)

From Figure 5-27 it can be observed that there is 94.30% chance of experiencing slight damage, 83.55% chance of experiencing moderate damage, 61.11% chance of experiencing extensive damage whereas complete damage has 29.62% chance of occurrence for a 5-storey building designed using gross section.

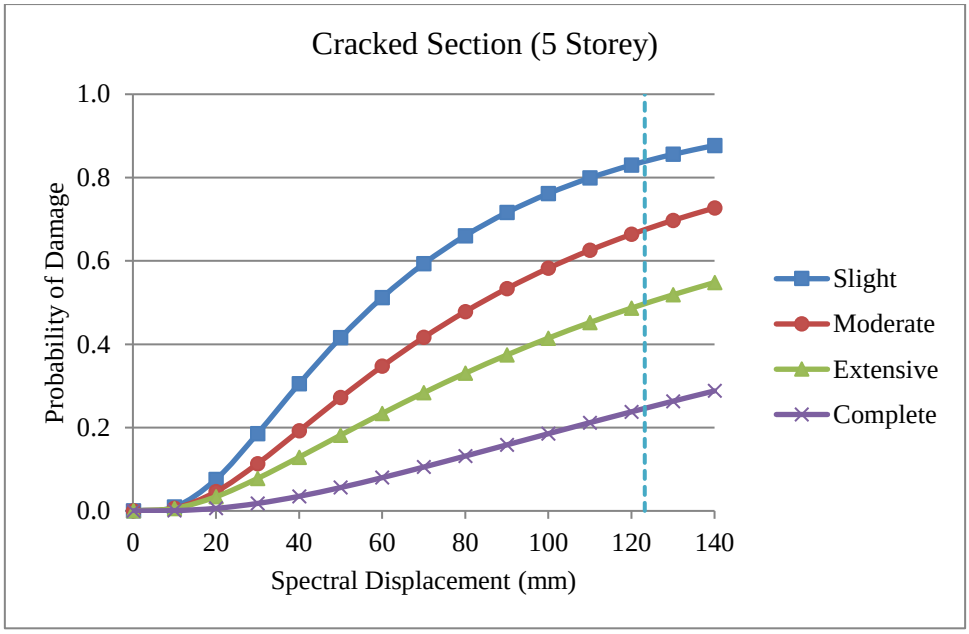

Figure 5-28 Fragility Curve for 5-storey model (Cracked)

Similarly, the probability of damage for cracked section model having 5 storeys was found to be 83.62%, 67.17%, 49.39% and 24.32% for slight, moderate, extensive and complete damage state respectively as shown in Figure 5-28.

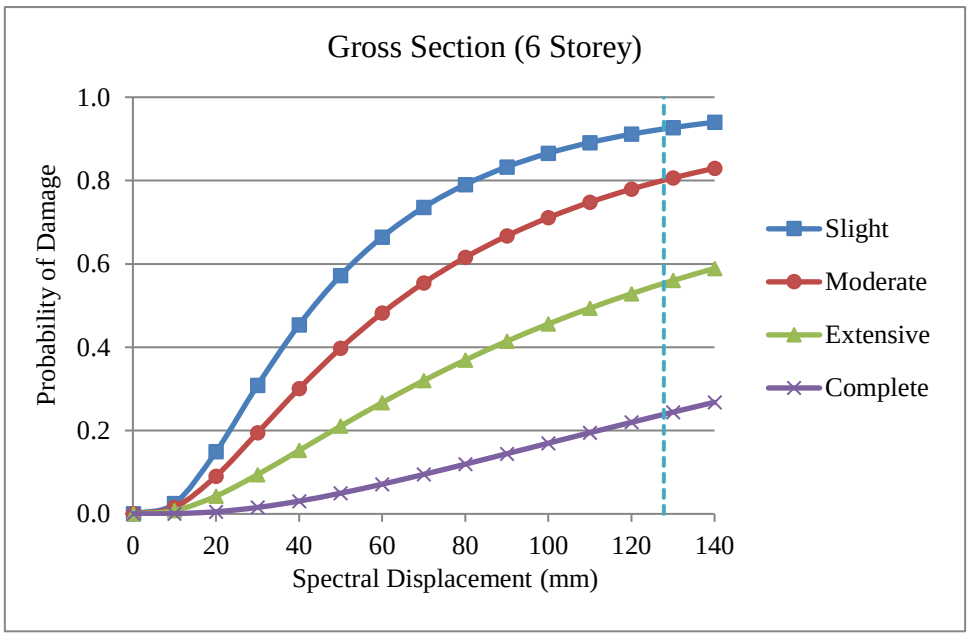

Figure 5-29 Fragility Curve for 6-storey model (Gross)

In a similar manner, the probability of damage for gross section model having 6 storeys was found to be 92.37%, 80%, 55.31% and 23.87% for slight, moderate, extensive and complete damage state respectively Figure 5-29.

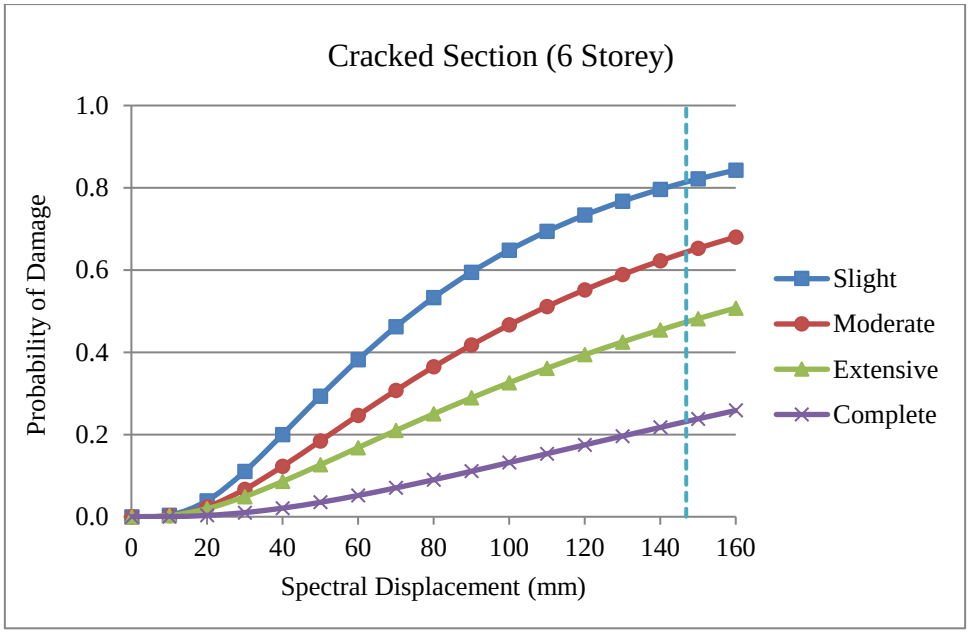

Figure 5-30 Fragility Curve for 6-storey model (Cracked)

From Figure 5-30 it can be observed that there is 81.35% chance of experiencing slight damage, 64.32% chance of experiencing moderate damage, 47.31% chance of experiencing extensive damage whereas complete damage has 23.15% chance of occurrence for a 6-storey building designed using cracked section.

Table 5-4 Discrete probability of exceeding damage states

No. of Storey	Analysis Case	Spectral Displacement at performance point (mm)	Damage States			
			Slight	Moderate	Extensive	Complete
2	Gross	43.67	0.146	0.246	0.293	0.196
	Cracked	55.47	0.161	0.189	0.259	0.225
3	Gross	90.76	0.104	0.191	0.304	0.350
	Cracked	102.23	0.196	0.218	0.155	0.327
4	Gross	91.79	0.095	0.250	0.336	0.272
	Cracked	113.30	0.172	0.265	0.181	0.291
5	Gross	112.46	0.107	0.224	0.314	0.296
	Cracked	123.20	0.164	0.177	0.250	0.243
6	Gross	127.80	0.123	0.247	0.310	0.238
	Cracked	146.89	0.170	0.170	0.241	0.231

Table 5-4 illustrates the discrete probability of exceeding the damage states for both gross and cracked section. For a building designed using gross section, the probability of exceeding damage states at the performance point is higher, particularly for the

moderate and extensive states, which reflects the higher effective damping values of gross sections which is also evident from the pushover analysis. It can also be observed that the gross section models undergo higher damage which is due to higher energy absorption whereas the cracked section model suffers less damage as it dissipates energy through large displacement. Hence, the overall damage on a scale of unity was found to be lesser for the cracked section.

Table 5-5 Probability of damage of buildings

Buildings	**Probability of damage (%)**				**Damage States**
	Slight	**Moderate**	**Extensive**	**Complete**	
2S5BG	88.32	73.65	49.02	19.62	Moderate
2S5BC	83.52	67.32	48.42	22.52	Moderate
3S5BG	95.17	84.70	65.52	35.08	Extensive
3S5BC	89.76	70.12	48.28	32.76	Moderate
4S5BG	95.52	85.97	60.93	27.26	Extensive
4S5BC	91.05	73.83	47.28	29.18	Moderate
5S5BG	94.31	83.56	61.11	29.62	Extensive
5S5BC	83.62	67.18	49.40	24.33	Moderate
6S5BG	92.37	80.04	55.31	23.87	Extensive
6S5BC	81.36	64.33	47.32	23.16	Moderate

From the fragility analysis of the buildings, the probability of damage at different damage states are determined which is tabulated in Table 5-5 in order to compare the results obtained. Analyzing these probabilities, the buildings designed using gross section were expected to have extensive damage whereas the buildings designed using cracked section were expected to have moderate damage.

CHAPTER 6: CONCLUSIONS

6.1 Conclusion

In this thesis, the impacts on the seismic performance of the RC frame buildings designed with variation in effective stiffness were studied. Basically, the modeling approach of the building in terms of gross stiffness and cracked stiffness was evaluated. A total of 40 models were developed in which the parameters that were varied were the number of storey and number of bays apart from the variation in effective stiffness.

Some of the major conclusions are as follows:

- Response of analyzed buildings show that the inter-storey drift and time period have been highly influenced when considering the gross and cracked section respectively.
- The seismic displacement demand for a building designed using cracked section is higher than a building designed using gross section, implying that cracked section modeling is more crucial.
- The gross section model overestimates ultimate capacity with a considerable margin of safety, which may not represent the real scenario of existing buildings as the cracks occur even due to the service loads.
- Cracked section models dissipate energy through large displacement, but uncracked sections resist it through higher initial stiffness, implying that cracked sections are more flexible as well as ductile.
- Gross section models are more susceptible to damage due to higher energy absorption whereas the cracked section models suffer less damage as it dissipates energy through large displacement which is evident from the results obtained from fragility analysis.

6.2 Recommendations for future works

- The effect of infill to reflect the real behavior can be considered.
- Soil site condition can be addressed by taking soil structure interaction into account.
- As this study only considers regular in plan and elevation low rise building, analysis can be carried out for irregular and high-rise building.

REFERENCES

ACI Committee 318 (2019). Building Code Requirements for Structural Concrete (ACI 318-19) and Commentary (ACI 318R-19), American Concrete Institute, 2019

Ahmed, M. (2008). Effect of concrete cracking on the lateral response of RCC buildings. Asian Journal of Civil Engineering (Building and Housing), 9(1), 25–34.

AIJ. (2010). Standard for structural calculation of reinforced concrete structures. Tokyo, Japan: Architectural Institute of Japan.

ASCE/SEI 41-13 Standard. (2013). American Society of Civil Engineers (ASCE). Seismic Evaluation and Retrofit of Existing Buildings, ASCE Standard No. ASCE/SEI 41-13, US.

Barbat, A. H., Pujades, L. G., & Lantada, N. (2008). Seismic Damage Evaluation in Urban Areas Using the Capacity Spectrum Method: Application to Barcelona. Soil Dynamics and Earthquake Engineering, 28, 851–865.

Branson, D.E. (1965). Instantaneous and time dependent deflections of simple and continuous reinforced-concrete beams. HPR Publications, 7(Part 1), Alabama Highway Department (Alabama, USA), U.S. Bureau of Public Roads.

Calvi, G. M., Pinho, R., Magenes, G., Bommer, J. J., Restrepo-Vélez, L. F., & Crowley, H. (2006). Development of seismic vulnerability assessment methodologies over the past 30 years. ISET Journal of Earthquake Technology, 43(3), 75–104.

Chaulagain, H., Rodrigues, H., Spacone, E., Guragain, R., Mallik, R., & Varum, H. (2014). Response Reduction factor of irregular RC buildings in Kathmandu Valley, Earthquake Engineering and Engineering Vibration. Vol. 13, pp. 455-470.

Elwood, K. J., & Eberhard, M. O. (2009). Effective stiffness of reinforced-concrete columns, ACI Struct. J. 106(4), 476-484.

EC8 UNI EN 1998-1-2005 (2005). Design of structures for earthquake resistance - Part 1: general rules, Seismic Actions and Rules for Buildings, Comité Européen de Normalisation, Brussels, Belgium.

FEMA 440. (2005). Federal Emergency Management Agency, Improvement of nonlinear static seismic analysis procedures, Washington D.C., US.

Federal Emergency Management Agency FEMA 356:2000 (2000), Prestandard and Commentary for the seismic rehabilitation of buildings, FEMA Publications No. 356, prepared by the American Society of Civil Engineers for the Federal Emergency Management Agency, Washington, USA.

FEMA/NIBS methodology HAZUS®-MH MR5 (2003). Advanced Engineering Building Module: Technical and User's Manual, Federal Emergency Management Agency, Washington D.C, USA.

Grossman, J.S. (1981). Simplified computations for effective moment of inertia and minimum thickness to avoid deflection computations, ACI J., 78(6),423-439.

Haldar, P., & Singh, Y. (2009). Seismic performance and vulnerability of Indian code designed RC frame buildings. ISET Journal of Earthquake Technology, 46(1), 29–45.

Halder, L., & Paul, S. (2016). Seismic Damage Evaluation of Gravity Load Designed Low Rise RC Building Using Non-linear Static Method. Procedia Engineering, 144, 1373–1380.

IS 1893 (2002). Criteria for earthquake resistant design of structures, Part-1 General Provisions and Buildings New Delhi: Bureau of Indian Standards.

IS 1893 (2016). Criteria for earthquake resistant design of structures, Part-1 General Provisions and Buildings New Delhi: Bureau of Indian Standards.

Kaushik, H. B. (2011). Importance of effective stiffness properties of rc members in seismic analysis and design of structures. Annals of the Indian National Academy of Engineering (INAE), 191–196.

Kaushik, H. B., & Mane, A. L. (2010). Effect of Cracked Section on Lateral Response of RC structures. 14th European Conference on Earthquake Engineering.

Khuntia, M., & Ghosh, S.K. (2004). Flexural stiffness of reinforced-concrete columns and beams: analytical approach, ACI Struct. J., 101(3),351-363.

Kumar, R., & Singh, Y. (2010). Stiffness of reinforced-concrete frame members for seismic analysis, ACI Struct. J., 107(5),607-615.

Mehanny, S. S. F., Kuramoto, H., & Deierlein, G. G. (2001). Stiffness modeling of R/C beam-columns for frame analysis. ACI Struct. J., 98(2),215-225.

Kwon, J., & Ghannoum, W. M. (2016). Assessment of international standard provisions on stiffness of reinforced concrete moment frame and shear wall buildings. Engineering Structures, 128, 149–160.

Miranda, E. (1993). Site-dependent strength-reduction factors. Journal of Structural Engineering 119(12), 3503–3519.

Miranda, E., & Bertero, V. V., (1994). Evaluation of strength reduction factor for earthquake-resistant design. Earthquake spectra10(2), 357-379

Mirza, S.A. (1990). Flexural stiffness of rectangular reinforced-concrete columns. ACI Struct. J., 7(4),425-435.

Monavari, B., & Massumi, A. (2012). Estimation of Displacement Demand in RC Frames and Comparing with Target Displacement Provided by FEMA-356. 15th World Conference on Earthquake Engineering (15WCEE).

Murty C. V. R., Rupen G., Vijayanarayanan A., Vipul V. M. (2012) Some concepts in earthquake behaviour of buildings. Gujarat State Disaster Management Authority.

Nepal National Building Code NBC 105:1994. (1994). Seismic Design of Buildings in Nepal.

Nepal National Building Code NBC 105: 2020. (2020). Seismic Design of Buildings in Nepal.

NZS 3101: Part 2 (2006). Concrete structures standard, Part 2 – Commentary on the design of concrete structures. Standards New Zealand, Wellington, NZ.

Pique, J. R., & Burgos, M. (2008). Effective Rigidity Of Reinforced Concrete Elements In Seismic Analysis and Design. 14th World Conference on Earthquake Engineering (14WCEE).

Prajapati, S. K., & Amin, J. A. (2019). Seismic assessment of RC frame building designed using gross and cracked section as per Indian standards. Asian Journal of Civil Engineering, 20(6), 821–836.

Priestley, M.J.N. (1998). Brief comments on elastic flexibility of reinforced concrete frames and significance to seismic design. Bull. of N.Z. Natl. Society for Earthq. Eng., 31(4):246-259.

Priestley, M. J. N. (2003). Myths and Fallacies in Earthquake Engineering , Revisited The Ninth Mallet Milne Lecture.

Rajbhandari, P. (2019), Response Reduction Factor for Seismic Design of Buildings in Nepal. MSc Thesis, Department of Civil Engineering, Tribhuvan University, Nepal.

Sugano, S. (1970). Experimental study on restoring-force characteristics of reinforced-concrete members. Dissertation, University of Tokyo, Japan.

Surana, M., Singh, Y., & Lang, D. H. (2015). Seismic performance of shear-wall and shear-wall core buildings designed for Indian codes. Advances in Structural Engineering: Dynamics, Volume Two, 43, 1229–1241.

Turkish Building Seismic Code (2018). Prime Ministry, Disaster and Emergency Management Presidency (AFAD), Ankara, 2018.

Wang, Q. (2001). Nonlinear stiffness design optimization of tall reinforced-concrete buildings under service loads. M.S. Dissertation, Hong Kong University of Science and Technology.

APPENDIX

Appendix 1: Inter-storey drift ratio

No. of storey	No. of bay	Elevation (m)	Gross		Cracked	
			ULS	SLS	ULS	SLS
2	2x2	6	0.00494	0.00119	0.00818	0.00196
		3	0.00559	0.00134	0.00872	0.00209
		0	0	0	0	0
	3x3	6	0.00517	0.00124	0.00846	0.00203
		3	0.0061	0.00146	0.00945	0.00227
		0	0	0	0	0
	4x4	6	0.0053	0.00127	0.0086	0.00207
		3	0.0064	0.00154	0.00987	0.00237
		0	0	0	0	0
	5x5	6	0.00538	0.00129	0.00868	0.00208
		3	0.0066	0.00159	0.01014	0.00244
		0	0	0	0	0
3	2x2	9	0.00494	0.00118	0.00863	0.00207
		6	0.00831	0.00199	0.0139	0.00333
		3	0.00648	0.00155	0.01038	0.00249
		0	0	0	0	0
	3x3	9	0.00497	0.00119	0.00855	0.00205
		6	0.00864	0.00207	0.01431	0.00343
		3	0.00695	0.00167	0.01105	0.00265
		0	0	0	0	0
	4x4	9	0.00497	0.00119	0.00848	0.00203
		6	0.00882	0.00211	0.01452	0.00348
		3	0.00722	0.00173	0.01143	0.00274
		0	0	0	0	0
	5x5	9	0.00496	0.00119	0.00842	0.00202
		6	0.00892	0.00214	0.01463	0.00351
		3	0.0074	0.00177	0.01167	0.0028
		0	0	0	0	0
4	2x2	12	0.00308	0.00074	0.00596	0.00143
		9	0.00574	0.00138	0.01074	0.00258
		6	0.00738	0.00177	0.01352	0.00324
		3	0.00542	0.0013	0.00928	0.00223
		0	0	0	0	0
	3x3	12	0.00309	0.00074	0.00591	0.00142
		9	0.00594	0.00143	0.01099	0.00264
		6	0.00774	0.00186	0.01404	0.00337
		3	0.00584	0.0014	0.00992	0.00238
		0	0	0	0	0

	4x4	12	0.00309	0.00074	0.00587	0.00141
		9	0.00604	0.00145	0.01112	0.00267
		6	0.00794	0.00191	0.01432	0.00344
		3	0.0061	0.00146	0.01029	0.00247
		0	0	0	0	0
	5x5	12	0.00308	0.00074	0.00584	0.0014
		9	0.00611	0.00147	0.01119	0.00269
		6	0.00806	0.00194	0.01449	0.00348
		3	0.00626	0.0015	0.01053	0.00253
		0	0	0	0	0
5	2x2	15	0.00348	0.00084	0.00661	0.00159
		12	0.00652	0.00156	0.01218	0.00292
		9	0.00896	0.00215	0.01674	0.00402
		6	0.01006	0.00241	0.01848	0.00443
		3	0.007	0.00168	0.01204	0.00289
		0	0	0	0	0
	3x3	15	0.00344	0.00082	0.00649	0.00156
		12	0.00666	0.0016	0.01235	0.00296
		9	0.00926	0.00222	0.01715	0.00411
		6	0.01052	0.00252	0.01916	0.0046
		3	0.00754	0.00181	0.01284	0.00308
		0	0	0	0	0
	4x4	15	0.0034	0.00082	0.00641	0.00154
		12	0.00674	0.00162	0.01243	0.00298
		9	0.00944	0.00226	0.01737	0.00417
		6	0.01078	0.00259	0.01954	0.00469
		3	0.00785	0.00188	0.01331	0.00319
		0	0	0	0	0
	5x5	15	0.00337	0.00081	0.00635	0.00152
		12	0.00679	0.00163	0.01248	0.00299
		9	0.00954	0.00229	0.0175	0.0042
		6	0.01094	0.00262	0.01976	0.00474
		3	0.00805	0.00193	0.01362	0.00327
		0	0	0	0	0
6	2x2	18	0.00327	0.00078	0.00635	0.00152
		15	0.00578	0.00139	0.01106	0.00265
		12	0.00803	0.00193	0.01541	0.0037
		9	0.00954	0.00229	0.01826	0.00438
		6	0.00978	0.00235	0.0183	0.00439
		3	0.0061	0.00146	0.01072	0.00257
		0	0	0	0	0
	3x3	18	0.00311	0.00075	0.00608	0.00146
		15	0.00576	0.00138	0.01099	0.00264

		12	0.00812	0.00195	0.01552	0.00372
		9	0.00974	0.00234	0.01854	0.00445
		6	0.01011	0.00243	0.01883	0.00452
		3	0.00648	0.00156	0.01132	0.00272
		0	0	0	0	0
	4x4	18	0.00303	0.00073	0.00594	0.00143
		15	0.00576	0.00138	0.01097	0.00263
		12	0.00819	0.00197	0.01559	0.00374
		9	0.00987	0.00237	0.01872	0.00449
		6	0.01032	0.00248	0.01915	0.0046
		3	0.00672	0.00161	0.01169	0.00281
		0	0	0	0	0
	5x5	18	0.00297	0.00071	0.00582	0.0014
		15	0.00574	0.00138	0.01093	0.00262
		12	0.00822	0.00197	0.01559	0.00374
		9	0.00993	0.00238	0.01878	0.00451
		6	0.01043	0.0025	0.0193	0.00463
		3	0.00686	0.00165	0.0119	0.00286
		0	0	0	0	0

Appendix 2: Time Period

No. of storey	No. of bay	Time Period (sec)		% Increase
		Gross	Cracked	
2	2x2	0.379	0.478	26.12
	3x3	0.392	0.492	25.51
	4x4	0.399	0.500	25.31
	5x5	0.404	0.504	24.75
3	2x2	0.492	0.633	28.66
	3x3	0.501	0.640	27.74
	4x4	0.506	0.644	27.27
	5x5	0.509	0.646	26.92
4	2x2	0.510	0.686	34.51
	3x3	0.519	0.694	33.72
	4x4	0.524	0.698	33.21
	5x5	0.527	0.701	33.02
5	2x2	0.654	0.883	35.02
	3x3	0.663	0.890	34.24
	4x4	0.668	0.894	33.83
	5x5	0.672	0.897	33.48
6	2x2	0.739	1.014	37.21
	3x3	0.743	1.014	36.47
	4x4	0.745	1.015	36.24
	5x5	0.747	1.015	35.88

Appendix 3: Calculation of Overstrength and Ductility:

Model	**V_d**	**d_u**	**d_y**	**V_y**	**Ω**	**μ**	**ϕ**	**R_μ**
2S2BG	167.68	109.79	24.43	655.35	3.908	4.493	1.283	3.722
2S2BC	167.68	128.71	39.05	653.69	3.898	3.296	1.096	3.094
2S3BG	337.03	108.02	23.84	1202.72	3.569	4.531	1.264	3.792
2S3BC	337.03	124.64	37.27	1187.59	3.524	3.345	1.079	3.172
2S4BG	563.87	106.62	23.68	1926.06	3.416	4.502	1.252	3.796
2S4BC	563.87	123.33	36.40	1882.97	3.339	3.388	1.069	3.231
2S5BG	848.21	107.05	23.71	2833.61	3.341	4.515	1.245	3.823
2S5BC	848.21	122.40	36.00	2747.87	3.240	3.400	1.065	3.253
3S2BG	271.01	142.30	30.72	746.99	2.756	4.632	1.120	4.241
3S2BC	271.01	174.59	49.91	736.58	2.718	3.498	0.919	3.717
3S3BG	541.47	140.06	31.48	1474.12	2.722	4.449	1.101	4.131
3S3BC	541.47	170.13	54.80	1583.61	2.925	3.105	0.904	3.326
3S4BG	903.01	137.84	34.69	2675.40	2.963	3.973	1.078	3.755
3S4BC	903.01	165.06	53.76	2563.34	2.839	3.070	0.900	3.299
3S5BG	1355.64	135.67	34.29	3943.41	2.909	3.957	1.074	3.751
3S5BC	1355.64	163.33	52.84	3757.32	2.772	3.091	0.898	3.326
4S2BG	412.31	174.96	33.57	1171.61	2.842	5.211	1.118	4.766
4S2BC	412.31	212.85	58.50	1129.14	2.739	3.638	0.874	4.016
4S3BG	821.65	168.43	33.93	2279.77	2.775	4.964	1.095	4.617
4S3BC	821.65	201.65	58.03	2188.11	2.663	3.475	0.864	3.861
4S4BG	1368.49	164.05	34.06	3721.26	2.719	4.816	1.083	4.522
4S4BC	1368.49	198.78	57.98	3602.37	2.632	3.429	0.860	3.821
4S5BG	2052.83	163.98	34.10	5527.17	2.692	4.808	1.079	4.529
4S5BC	2052.83	195.95	57.77	5348.15	2.605	3.392	0.857	3.788
5S2BG	521.93	209.20	46.35	1259.08	2.412	4.513	0.923	4.802
5S2BC	521.93	258.67	81.54	1215.87	2.330	3.172	0.761	3.853
5S3BG	1040.58	203.79	46.98	2483.78	2.387	4.338	0.910	4.664
5S3BC	1040.58	252.66	83.01	2434.89	2.340	3.044	0.757	3.697

Model	V_d	d_u	d_y	V_y	Ω	μ	ϕ	R_μ
5S4BG	1733.60	201.66	47.91	4122.21	2.378	4.209	0.903	4.553
5S4BC	1733.60	248.71	82.49	4001.81	2.308	3.015	0.756	3.664
5S5BG	2601.01	197.87	47.86	6198.91	2.383	4.134	0.897	4.491
5S5BC	2601.01	244.87	83.79	6070.50	2.334	2.923	0.754	3.548
6S2BG	588.43	277.87	60.32	1577.16	2.680	4.606	0.856	5.211
6S2BC	588.43	336.39	107.76	1525.28	2.592	3.122	0.743	3.855
6S3BG	1169.05	267.69	62.50	3199.99	2.737	4.283	0.845	4.880
6S3BC	1169.05	320.42	110.48	3112.61	2.663	2.900	0.740	3.566
6S4BG	1944.21	252.76	62.72	5429.17	2.792	4.030	0.839	4.610
6S4BC	1944.21	308.98	114.41	5365.19	2.760	2.701	0.737	3.304
6S5BG	2913.91	260.00	62.34	8047.66	2.762	4.171	0.840	4.770
6S5BC	2913.91	305.89	107.43	7544.66	2.589	2.847	0.739	3.497

Appendix 4: Fragility analysis

Buildings	Spectral displacement at performance point (mm)	Probability of damage (%)				Damage States
		Slight	Moderate	Extensive	Complete	
2S2BG	34.022	79.78	63.08	38.60	13.24	Moderate
2S2BC	42.838	70.90	53.64	36.42	14.73	Moderate
2S3BG	37.558	83.96	67.98	43.05	15.72	Moderate
2S3BC	46.152	75.79	58.62	40.52	17.19	Moderate
2S4BG	41.532	87.25	72.09	47.33	18.45	Moderate
2S4BC	50.934	80.56	63.74	44.94	19.97	Moderate
2S5BG	43.665	88.32	73.65	49.02	19.62	Moderate
2S5BC	55.465	83.52	67.32	48.42	22.52	Moderate
3S2BG	83.311	95.42	85.24	63.04	30.48	Extensive
3S2BC	109.5	92.34	79.58	51.22	32.87	Extensive
3S3BG	87.173	95.67	85.75	64.66	32.55	Extensive
3S3BC	101.408	88.75	74.12	46.54	31.10	Moderate
3S4BG	88.13	94.60	83.63	63.96	33.49	Extensive
3S4BC	101.735	89.27	74.86	47.54	32.23	Moderate
3S5BG	90.76	95.17	84.70	65.52	35.08	Extensive
3S5BC	102.23	89.76	70.12	48.28	32.76	Moderate
4S2BG	89.063	96.19	87.41	60.09	24.97	Extensive
4S2BC	119.219	92.27	79.87	47.68	28.11	Moderate
4S3BG	94.152	96.64	88.43	62.93	28.02	Extensive
4S3BC	116.188	91.89	79.24	47.71	29.06	Moderate
4S4BG	94.68	96.65	88.47	63.70	29.11	Extensive
4S4BC	113.849	91.50	78.58	47.16	28.85	Moderate
4S5BG	91.789	95.52	85.97	60.93	27.26	Extensive
4S5BC	113.296	91.05	73.83	47.28	29.18	Moderate
5S2BG	117.519	95.66	86.27	61.75	28.20	Extensive
5S2BC	127.033	85.65	69.86	49.00	23.85	Moderate
5S3BG	115.035	95.21	85.34	61.31	28.36	Extensive
5S3BC	124.81	84.54	68.38	49.77	24.03	Moderate
5S4BG	114.37	94.86	84.64	61.02	28.52	Extensive
5S4BC	124.056	84.55	68.39	49.97	24.33	Moderate
5S5BG	112.459	94.31	83.56	61.11	29.62	Extensive
5S5BC	123.202	83.62	67.18	49.40	24.33	Moderate
6S2BG	130.046	93.32	81.69	54.99	22.38	Extensive

Buildings	Spectral displacement at performance point (mm)	Probability of damage (%)				Damage States
		Slight	Moderate	Extensive	Complete	
6S2BC	139.942	79.50	62.07	43.48	19.02	Moderate
6S3BG	127.445	92.27	79.87	54.48	22.90	Extensive
6S3BC	140.231	78.62	61.04	44.03	20.43	Moderate
6S4BG	120.353	91.05	77.83	53.50	22.90	Extensive
6S4BC	139.968	77.17	59.37	43.93	21.42	Moderate
6S5BG	127.795	92.37	80.04	55.31	23.87	Extensive
6S5BC	146.886	81.36	64.33	47.32	23.16	Moderate